DEPARTMENT OF BIOENGINEERING

VISUAL PATHOLOGY RECTIFICATION

by

DUSHYANTH GOPICHAND (201169716)

THIS THESIS IS SUBMITTED IN PARTIAL FULFILMENT OF THE REQUIREMENTS FOR THE DEGREE OF MSC IN BIOENGINEERING

SEPTEMBER-2012
BIOENGINEERING UNIT
UNIVERSITY OF STRATHCLYDE
GLASGOW, UK

DECLARATION OF AUTHENTICITY AND AUTHOR'S RIGHTS

This thesis is the result of the author's original research. It has been composed by the author and has not been previously submitted for examination which has led to the award of a degree.

Sign:

Date:

ACKNOWLEDGEMENTS

I am very grateful to his, The Almighty God for giving me the knowledge and power to complete this thesis.

I sincerely thank my supervisor Prof William Sandham for his support, vision and knowledge, without which this thesis would not be possible. I would also like to record my appreciation to Dr David Hamilton, CEO Ateeda Ltd, for his insight in devising this project in the first place.

I thank all my colleagues and friends who helped me in completing this thesis.

Lastly, I thank my parents, who always supported and stood beside me.

ABSTRACT

Human beings mostly rely on vision for most of the daily activities; any deformity in vision can limit a person's actions. These visual impairments can be genetic or age-related. Many individuals with a low and high-order visual problem find it hard to use a computer, even with the use of corrective lens, which can lower the self-esteem of an individual, as the use of computers have increased over the years. In this project, an algorithm was designed using a user's wave aberration in the eye, this aberration is used to generated the Point Spread Function (PSF) of the eye. The PSF describes the degree of spreading of an image at the focal point, hence it is a measure for the quality of an optical system. This PSF can be used as an impulse response to blur an image, and the image is recovered back using the same PSF by a deconvolution procedure. This processed image is presented to the user. Another possible method is the use of geometric optics. Optics describe the properties of a ray of light as it propagates through an optical system. These properties are described in a transfer matrix, which is then used to improve an image for a visual impaired user. Results show that while viewing the screen, using Fourier optics method of compensation, alters the image that can be seen by a visual impaired person. On the other hand the results obtained from the geometrical optics do not modify the image as per the user requirements.

Table of Contents

LIST OF FIGURES

"Being disabled should not mean being
disqualified from having access to every aspect of life".

- *Emma Thompson*

1. INTRODUCTION

1.1 BACKGROUND

According to the World Health Organisation (WHO) there are about 285 million people worldwide, who suffer from visual impairment, and 90% of all visual impaired population live in developed countries. The organisation also claims that uncorrected refractive errors such as myopia – commonly referred as nearsightedness, is a condition where an individual has trouble focusing objects that are far away, which makes distant objects appear to be blurred; hyperopia – commonly known as farsightedness, where an individual with this condition will have difficulty seeing near objects; and astigmatism – is a condition in which vision is blurred due to inability of the eye to focus an object on the retina. All these refractive errors accounts for 43% of all visual impairments, and 80% of all visual impairment can be cured by corrective lens ("Visual Impairment and blindness", 2012). The National Health Service (NHS) state, 20%-30% of the children in the UK suffer from myopia and about two thirds of people over the age 65 have problems with sight ("Statistics and data collections", 2012 , "Visual Impairment and blindness", 2012).

Eyes provide sense of the vision and sight to humans and they also help an observer to interact with the world and electronics machines, such as computers. If there are any aberrations in the visual system (eye) of a user, it may affect the sight and the way user interacts with these machines, with in turn hinders a person's day to day actives. Hence, a computer display can be developed, which can modify the image displayed on the screen, so that an impaired person would be able to see. This thesis mainly concerns with the development of one such display system for a person with a refractive error.

One way to correct the refractive error is the use of optical lens, which was the only way available from past 13th century. Contact lens was introduced in the year 1949; which was first developed by Norman Gaylord ("New Contact Lens Fits Pupil Only", 1952), these lens fit the cornea of the user. This lens fit the cornea and correct any refractive error in the user, such as myopia or hyperopia. Contact lenses are very uncomfortable for the user and cause dryness in the eye (Chuang et al, 2008). Recent development in Laser technology has made it possible for, Laser–Assisted in-Suit Keratomileusis (LASIK); which is a laser eye surgery to correct the myopia, hyperopia and astigmatism. In this surgery, a low intensity laser ranging from 200nm-250nm wavelength is used to shape the cornea which increase visual acuity of the eye (McFadden, 2005). This is the only method to correct the refractive error of a person permanently. However, the cost of this surgery is high and mostly not feasible for the general public, and possesses many post-surgery complications such as extreme dryness in the eye, reduced lens-corrected visual acuity, double vision, light sensitivity and Epithelium erosion (Ambrosio et al, 2008).

This thesis presents two simple and effective methods that can be applied to correct the refractive error of an individual. One of the methods is to filter the image using the transfer matrix that describes the refraction of the ray of light in an optical system. The transfer matrix is derived by assuming the ray to be paraxial.

In the second method, the wavefront aberration function is used to determine the aberration in the eye, this aberration is used to blur the image by using Fourier optics techniques, and this blurred image is then deconvoluted with the PSF (Point Spread Function) of the user's eye, thereby transforming the image suitable for the observer.

The advantages of the above mentioned procedure are that both methods do not require any additional bulky equipment and have zero infection risk. The user needs to know his wavefront aberration function; once the spherical wave aberration function is entered by the user the algorithm alters the computer display or an LCD (Liquid Crystal Display) display, and forms an image appropriate for the user.

1.2 AIMS AND OBJECTIVES

The use of computers has drastically increased over the few years, and humans are now living in an era where computers play a very important role in one's life. These electronics devices are designed on the base of user interfaces. These are a set of menus or commands on a computer display which enables the use to interact with the machine. A person with visual impairment will find these device's difficult to use. Thus, a new display scheme is required which makes it easier for an impaired vision person to use these smart devices. The objective is to develop an algorithm that can filter an image, and enable it to be seen by an impaired user while using a computer.

1.3 OVERVIEW OF THESIS

Chapter 2, gives an introduction to the anatomy and the physiology of the human eye. Chapter 3 gives an introduction to digital image processing and covers different image processing techniques that can be applied to an image.

Chapter 4 familiarise the reader with different approaches that could be used to process a digital image and their applicability to filter an image, so that it can be seen by a low-order visual impaired person. The two possible approaches that could be used to alter the image for a refractive error user are discussed in Chapter 5. Chapter 6 presents the practical implementation of these two methods. Finally, conclusions and possible extensions of this research are suggested in Chapter 7.

"The eyes are extremely sophisticated visual instruments-more versatile and adaptable than the most expensive cameras, yet compact and durable."

- *Frederic H. Martini, in this book – "Fundamentals of Anatomy & Physiology"*

2 ANATOMY OF THE HUMAN EYE

The eyes are complex anatomical structures, which can detect light and provide us with the power of sight. The eyes give a three-dimensional view of the world. Each eye is a slightly irregular spheroid with an average diameter of 24 mm. Within the orbit, the eyeball shares the space with the extrinsic eye muscles, the lacrimal gland, the cranial nerves and the blood supply to the eye. A thin layer of orbital fat, cushions and insulates the eye (Martini et al, 2009).

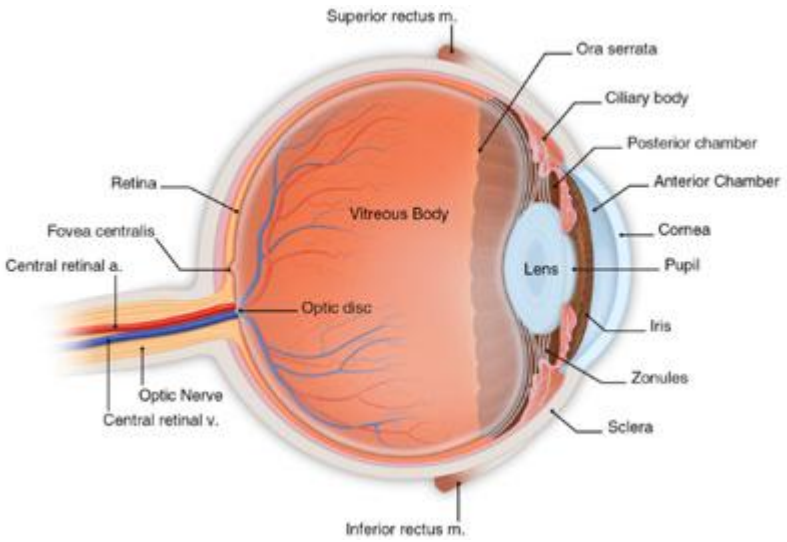

Figure 2-1 Sagittal section of the left eye (Campbell, 2006).

The eye contains three layers or tunics: 1) an outer fibrous tunic, 2) an intermediate vascular tunic, and 3) an inner neural tunic (retina)-which consists of photoreceptors. The eyeball is hollow, and its interior is divided into two cavities - a large posterior cavity or vitreous chamber; named because it contains the gelatinous vitreous body

and a smaller anterior cavity which is filled by aqueous humor. The sagittal section of the eye showing all the inner organelles is shown in figure 2-1.

2.1 THE FIBROUS LAYER

The fibrous tunic forms the outermost layer of the eye. It consists of the sclera and the cornea. Sclera covers most of the ocular surface which is also referred as ‘white of the eye’; which contains a dense fibrous connective tissue including both collagen and elastin. This layer is thinnest at the anterior surface and thickest at the posterior surface side of the eye. This layer is connected by six extrinsic eye muscles which control the eyeball movement. This film is also lined with a network of blood vessels and nerves that penetrate the sclera to reach inner structures; see figure 2.1.

The cornea, a thin outer layer of the eye, is completely transparent and structurally continuous with sclera; the border between the two layers is called the corneal limbus. This layer is made of a dense matrix containing multiple layer of collagen fibers, organised in a way that does not interfere with passing light. This surface has no blood vessels, however oxygen and nutrients are supplied by the tear. Damages to the cornea can cause complete blindness, even though functional components of eye-photoreceptors are perfectly normal, hence injuries to the cornea should be treated immediately to prevent serious vision losses.

2.2 THE VASCULAR LAYER

The vascular tunic, or uvea, contains numerous blood vessels, lymphatic vessels and the intrinsic muscles of the eye; and it mainly constitutes the iris, the ciliary body and the choroid.

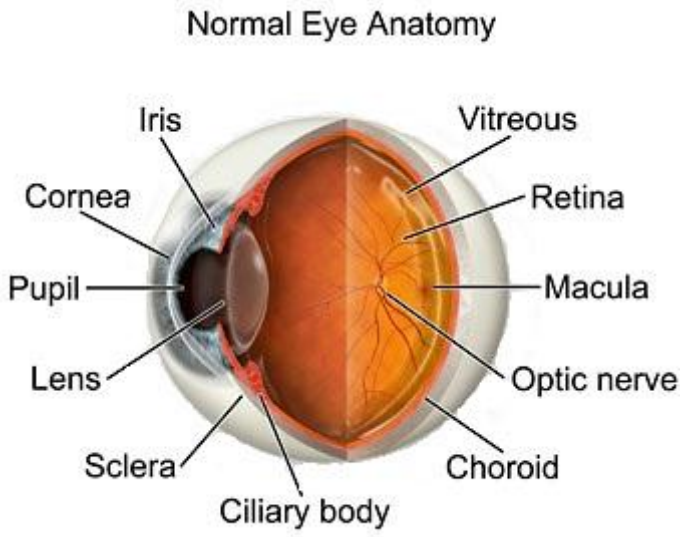

Figure 2-2 Anatomical structure of the eye (Generic Look.com, 2012)**.**

2.2.1 The Iris:

The iris is visible through the transplant corneal surface. It contains pigment cells and two layers of smooth muscle fibers. The smooth muscles are divided into pupillary constrictor muscles and pupillary dilator muscles. The iris also encloses a network of blood vessels, shown in figure 2-2.

When pupillary muscles contract they change the diameter of the pupil, which in turn regulate the amount of light entering the eye. The contraction is controlled by the autonomic nervous system; parasympathetic activation will cause the pupil to constrict in response to the brightness and sympathetic activation will dilate the pupil in dim light.

The iris is highly vascular, pigmented and lined with connective tissue. The epithelial tissue are absent on the anterior surface of the iris; instead it has an incomplete layer of fibrocytes and melanocytes. The posterior surface is covered by a pigmented epithelium that is a part of the neural tunic and mainly contains melanin granules. The colour of the eye is determined by the genes that influence the distribution and

density of melanocytes that are present on both the anterior and interior surfaces of the iris, and also the density of pigmented epithelium. When there are fewer melanocytes in the connective tissue, this give a lighter colour such as blue, and as the number of melanocytes increases, the eye colour becomes darker; black being the maximum number of melanocytes and the colour brown and green with a decreased number of melanocytes.

2.2.2 The Ciliary Body:

The iris is attached to the anterior portion of the ciliary body. These muscles extent posteriorly to reach ora serrate. The bulk of ciliary body consists of ciliary muscle, a smooth muscle ring that projects into the interior of the eye. These muscles are covered with epithelial tissue, which has numerous folds called ciliary process. The suspensory ligaments of the lens are attached to these processes. The connective-tissue fibers of these ligaments hold the lens posterior to the iris and centred on the pupil.

2.2.3 The Choroid:

Choroid is a vascular layer that separates the fibrous and neural tunics, that is present posterior to the ora serrate. It is covered by sclera and attached to the outermost later of the retina. Choroid contains a large network of capillaries that deliver oxygen and nutrients to retina.

2.3 THE NEURAL LAYER (RETINA)

The innermost layer of the eye is called the neural tunic or retina, which is made up of a thin outer layer called the pigmented part and a thick outer layer called the neural part. The pigmented part of the retina absorbs all the light that pass through upper layers and prevents any light bouncing back to these upper layers that can cause visual echoes. The pigment cells are equipped with light receptors that undergo biochemical interactions when a ray of light falls on these cells; these light receptors are located in the neural part of the retina. Additionally, the neural part of the retina

also contains supporting cells and neurons that can perform preliminary processing and integration of visual information.

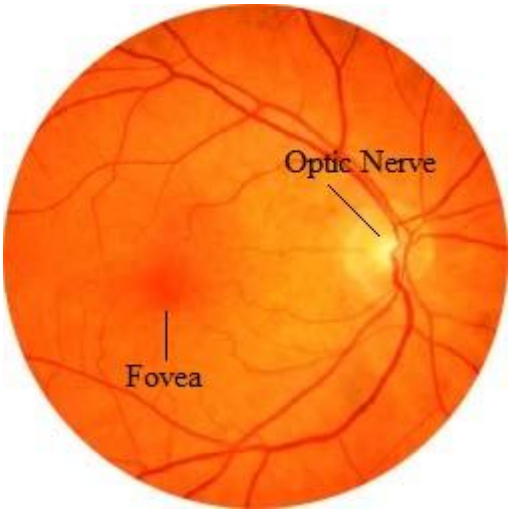

Figure 2-3 View of the retina through an ophthalmoscope (James, 2010).

2.3.1 Retina:

The outermost wall of the retina is lined with pigmented cells, which contains photoreceptors, or cells that detect light. These photoreceptors are further classified into two types: rods and cones. An Ophthalmoscope image of a healthy retina is shown in figure 2-3.

- Rods do not recognise different colours of the light, but they are highly sensitive to light, which enables human beings to see at twilight.
- Cones on the other hand are of three different types; each cone responds one of three colours of light: red, green and blue. For example red cones are activated when a red light is incident on the retina. Thus, simulation in various combinations provides the perception of colours, hence they give colour vision. Cones give shaper and clearer image then rods do, however cones need intensive light stimulation.

Rods and cones are not evenly distributed across the outer surface of the retina. There are approximately 125 million rods which are distributed across the periphery, and the density of rods gradually reduces at the centre of the retina. In other words, most of 6 million cons are concentrated in the centre of the retina, called the fovea. The basic structure of a rod and cone is shown in figure 2-5.

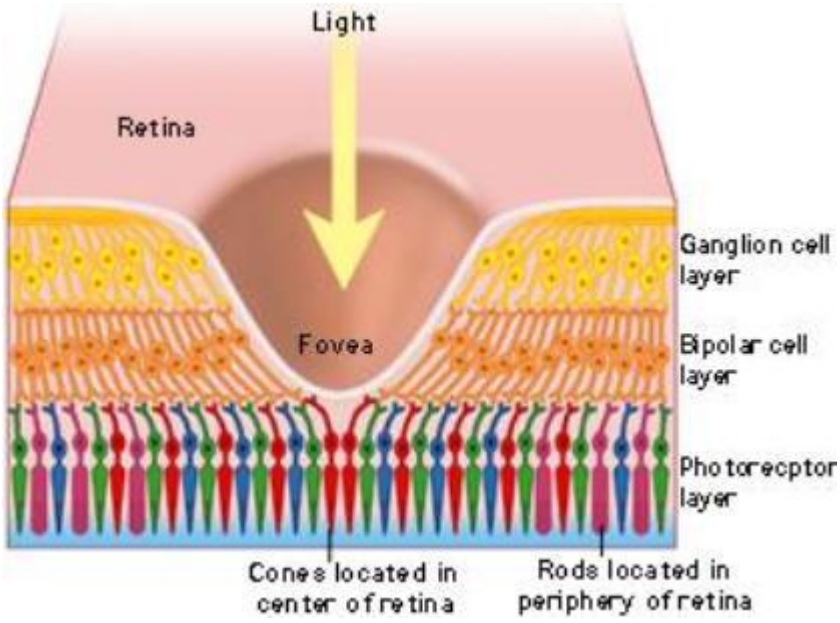

Figure 2-4 Organisation of cones and rods in the retina at the fovea (Budowa, 2008).

2.3.2 Macula Lutea:

Macula lutea is situated roughly at the centre of the retina and focuses the incoming light on to the fovea, resulting in central vision. This region does not contain any rods; as a result it is highly concentrated with cones. The centre of macula lutea is called Fovea, which has the highest concentration cones. An imaginary line drawn from the centre of the object to the fovea via the lens, establishes the visual axis of the eye. Figure 2-4 shows the Fovea region in the retina, with the organisation of cones.

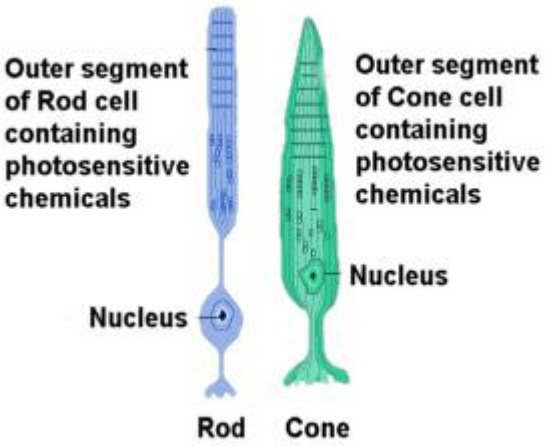

Figure 2-5 Structure of a rod and a cone in the retina (Mason, 2008).

2.3.3 The Optic Nerve:

This nerve transmits visual information in the form of electrical impulses from the retina to the brain. The optic disc provide a window for the optic nerve to enter the eye, and from this point the axons of the nerve turn and penetrate the wall of the eye and proceed towards the optical chiasm. The disc is present on the posterior part of the eye, very close to macula lutea, in fact in the same plane as of macula lutea. The optic disc has no photoreceptors, so a ray of light striking this area does not get noticed; therefore the optic disc is commonly referred to as a blind spot. However, this blind spot is normally not noticeable in the perceived field of vision primarily because involuntary eye movements keep the eye moving which allow the brain to fill the missing detail.

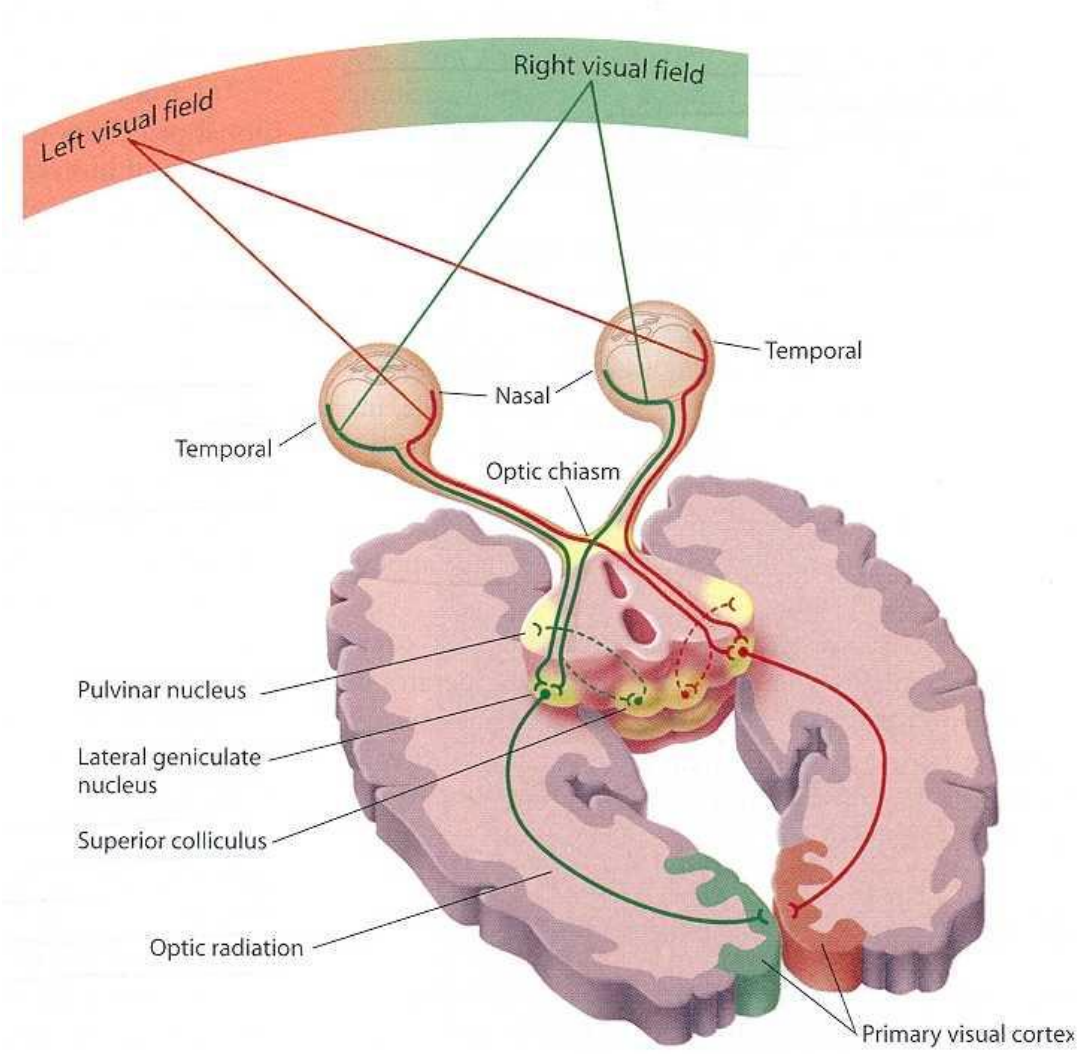

Figure 2-6 Path of the optic nerve from the eye to the cerebral cortex (visual pathway, 2011).

2.3.4 The Vitreous Body:

A gelatinous mass on the posterior cavity of the eye is called the vitreous body. It helps to stabilise the shape of the eye, otherwise the extraocular muscles will disorder the shape; because these muscles constantly change the orbit of the eye ball. The vitreous body contains many specialised cells that can secret collagen fibers and proteoglycans which accounts for consistency of gelatinous mass. These are formed during the development of the eye and are not replaced.

2.3.5 The Lens:

The lens lie posterior to the cornea, they are held in place by suspensory ligaments that emerge from ciliary body of the choroid. The primary function of the lens is to focus the light from the object on to the photoreceptors of the retina or fovea. The lens is made up of well organised, concentric cells. A dense elastic fibrous capsule covers the entire lens. The cells which are inside the lens are termed as lens fibers. These are highly specialised cells, which have lost their nuclei and other organelles and are filled with a transparent protein called crystallins that accounts for both clarity and focusing power of the lens. Additionally these proteins is very stable, hence the lens remain intact and are able to function for entire life time without the need for replacement. The transparency of the lens depends mainly on the structural and biochemical characteristics; when this is disturbed the lens loses its transparency; leads to an abnormality know as cataract.

2.4 OPTICS OF THE EYE

Light enters through the cornea, which is the smooth, tough and transparent surface of the eye. The amount of light reaching the retina is controlled by the pupil, which also helps in altering the numerical aperture of the eye's imaging system. Light gets focused by the lens, traverses into the liquid filled space called vitreous humour, and finally strikes the retina.

2.4.1 Refraction of the Light:

As mentioned before, the retina is lined with photoreceptors, that are about 130 million spread all over the surface expect the anterior potion of the retina. Each photoreceptor monitor the light that striking a specific area of the retina. The information received from these photoreceptors result in a visual image in the brain, this is accomplished only when the photoreceptors send useful information to the brain via the optic nerves. The lens plays an important role in focusing the rays of light arriving from the object. The rays must strike the sensitive surface of the retina or photographic film in a precise order so that a miniature image of the object is formed on the film. If the light is not focused properly then the image is blurred.

Light gets refracted when it travels from one medium to another medium (Poon et al, 2006). This is also applicable to the human eye. When a ray of light travels from air (rarer medium) to eye (denser medium), the light ray bends or is refracted, in the human eye, greatest amount of refraction occurs at the cornea tissue because the density of this tissue is very close to water. The travelling light is again refracted by the dense lens, which focuses the ray to form an object at the focal point. The distance between the centre of the lens to the focal point is called focal distance. The focal distance is determined by two factors:

- Distance of the Object: if the object is close to the lens, then the focal distance increases and if the object is far away from the lens, the focal distance decreases.
- Shape of the Lens: the rounder the lens, the more refraction occurs and hence the shorter the focal distance. A flatter lens gives less refraction which increase the focal distance.

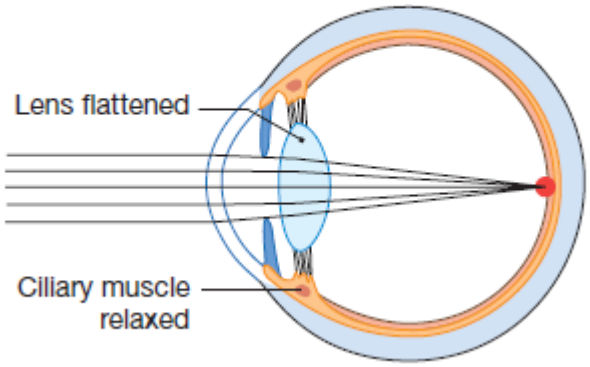

Figure 2-7 Lens flattened to focus distant objects (Martini et al, 2009).

The distance between the lens and macula lutea does not change; hence the image is focused on to the retina by the shape of the lens, keeping the focal length constant. This process is termed as accommodation. During this process, the lens become more spherical to focus an object close to the eye, and the lens flatten to focus a distant object.

As stated before the lenses are held by suspensory ligaments that are derived from ciliary body. The smooth muscles which exist in the ciliary body act like sphincter

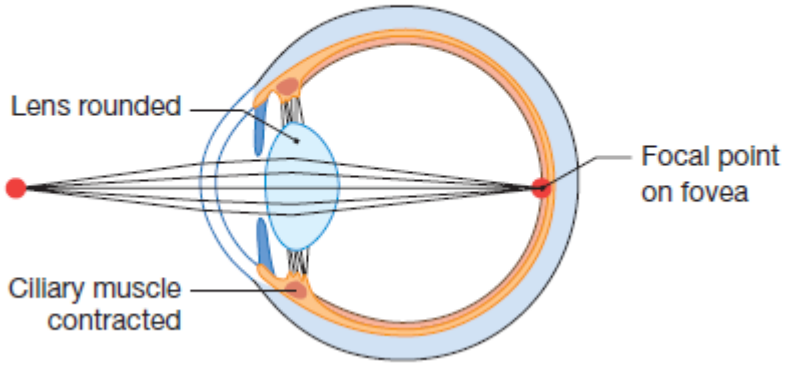

Figure 2-8 Lens becomes spherical to focus near objects (Martini et al, 2009).

muscles. When ciliary muscles contract, the ciliary body move towards the lens there by reducing the tension in the ligament, as a result the lens become more spherical in shape-increases the refractive power of the lens shown in figure 2-8 and when these muscles relax, the ligaments pull the circumference of the lens making it flatter-decreasing the refractive power of the lens shown in figure 2-7. Great amount refraction is needed to view an object that is very close to the eye.

Astigmatism is a condition in which the lens loses its refractive power as a result the lenses are unable to refract the incident light, even though the cornea is able to refract the light, hence visual image is distorted. Many individual suffer with minor astigmatism; the image distortion so minimum it is usually unnoticed in many condition.

2.4.2 Image Formation:

Let an object be considered to be made up of numerous points, when an object is viewed, all of these points can be treated as individual points that transmit light. Light from each of these points are focused on to the retina, as a result a miniature inverted image is formed on the retina screen. To understand why the image is reversed, consider looking at the tall telephone pole, the image on the top of the pole ends up landing at the bottom of the retina, and the base of the pole lands at the top surface of the retina, shown in figure 2-9. Hence the image is reversed on the retinal film. Now, consider looking at a horizontal fence, the image on the left edge falls on the right side of the retina and the image on the right-most section of the fence falls on the left side of the retina, shown in figure 2-10. The brain compensates this reversal of the image and perceives that the object is not inverted.

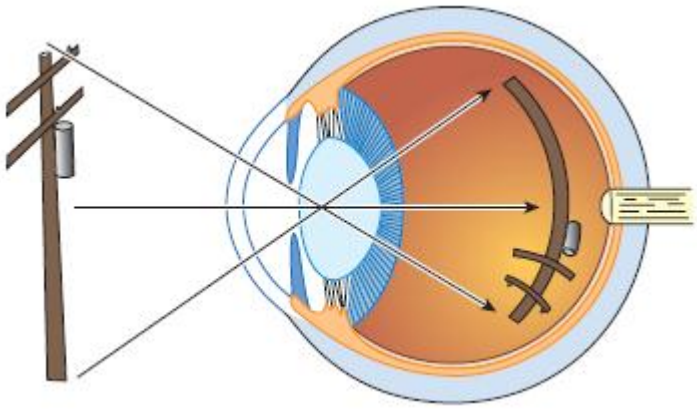

Figure 2-9 Image formed of a vertical object (Martini et al, 2009).

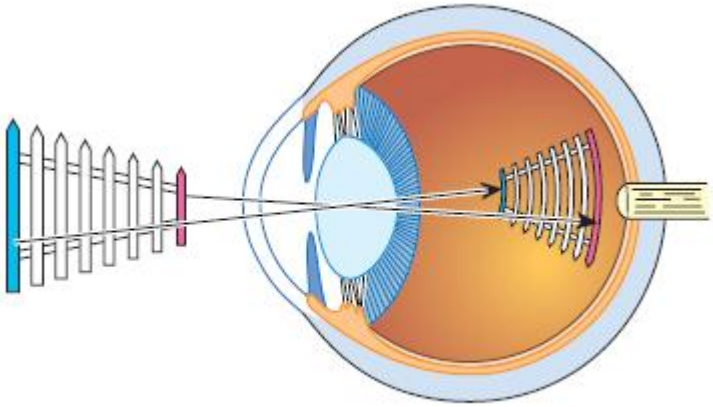

Figure 2-10 Image formation on the retina of a horizontal object (Martini et al, 2009).

2.4.3 Visual Acuity:

Visual Acuity is defined as the clarity or clearness of vision, which denotes the sharp focus of the image by the lens onto the retina. The standard vision rating of 6/6 denotes the level of details seen at a distance of six meters, by an individual with normal vision. If the visual acuity falls below 6/60, even with the help of a corrective lens, then an individual is considered to be blind ("Visual Impairment and blindness", 2008).

2.4.4 Refractive Error:

If the lenses are unable to focus the light from an object, then this results in a blurred image seen by an individual. This is known as the refractive error. This condition is commonly treated by adding an extra corrective concave or convex lens depending on the refractive error type. If the lenses are able to focus both distant object and a

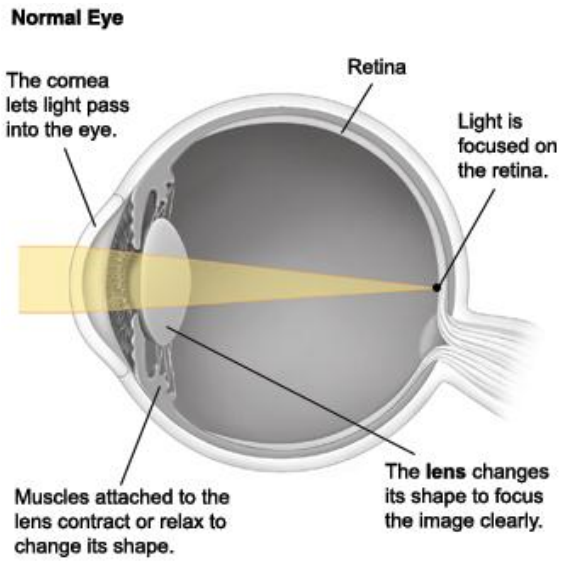

Figure 2-11 Normal eye focuses the image onto the fovea (Mount Nittany Health, 2009).

near object on to the retina, without any blurring of the image, then this condition is known as emmetropia or normal vision of a healthy human being, shown in figure 2-11. The two types of refractive error discussed here are myopia and hyperopia.

2.4.5 Myopia

Myopia is also termed as nearsightedness. A person with myopic condition will not be able to see distant objects, because light from the distant object appears to be fuzzy. This is because the cornea and lens bend the ray of light at a much higher angle; which in turn focuses the light in front of the retina in figure 2-12. However, objects that are close to the eyes are focused to the fovea of the retina, hence close objects appear crisp and clear.

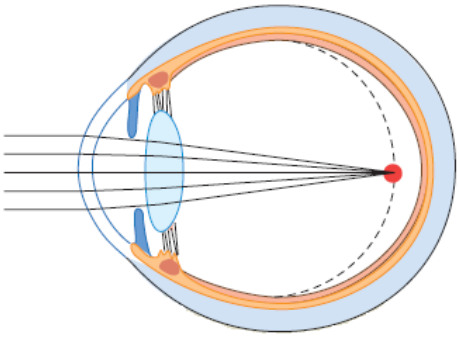

Figure 2-12 Eyes elongate- as a result an image is formed in front of the retina (Martini et al, 2009).

There are two types of Myopia:

- Axial Myopia: in the case of axial myopia, the eye elongates horizontally increasing the diameter, due to this enlargement of the eye, the object is incorrectly focused, and hence a fuzzy image is sent to the brain.
- Refractive Myopia: in this type of myopia, the cornea or the lens increases, due to this, the rays are refracted at much greater angle; resulting in an disfigured image to the observer (Wilson et al, 1989).

Both the above types of myopia can be treated by using a concave or diverging lens. The concave lens diverge the rays before it enters the eyes. Since now a pre-refracted diverge rays are incident on the lens-focus the image on the fovea of the retina. Therefore a clear image is formed on the retinal screen – figure 2.13.

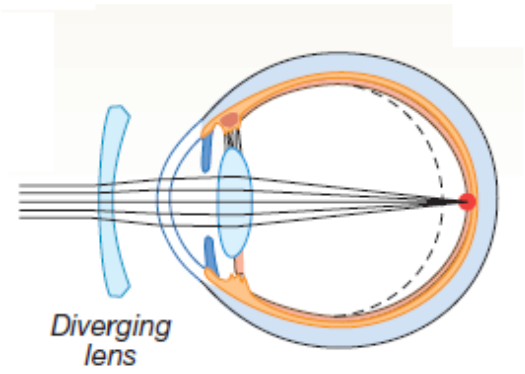

Figure 2-13 Myopia corrected by a diverging concave lens (Martini et al, 2009).

2.4.6 Hyperopia

Hyperopia is termed as farsightedness. In this condition the eyes are unable to focus objects that are close to the eye. When light rays are incident on the surface of the cornea and lens, the ray is bent at a very low angle and the image is formed behind the retina, shown in figure 2-14.

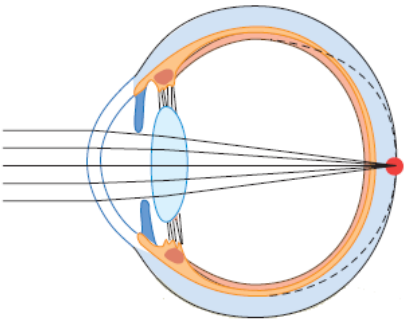

Figure 2-14 Hyperopia, eyes shorten hence image is formed behind the retina (Martini et al, 2009).

The eyes are shrunk, decreasing the diameter of the eyeball and also ciliary muscles lack the ability in making the lens spherical; this combined effect cause hyperopia. In other words the eyeball is small when compared to the curvature of the lens.

Hyperopia can be corrected by using a convex lens or a converging lens. The convex lens bends the plane light waves from the object before it enters the human optical system. This extra bending added by the convex lens will ultimately focus the image onto the fovea, in figure 2-15.

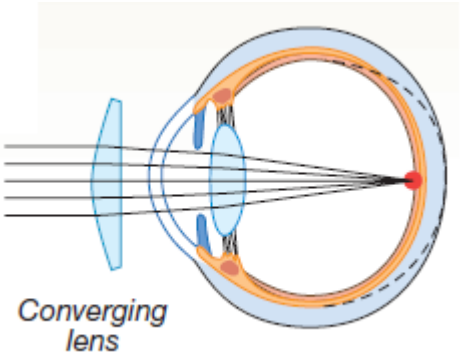

Figure 2-15 Hyperopia corrected using converging lens or convex lens (Martini et al, 2009).

"Any sufficiently advanced technology is indistinguishable from magic"

- *Arthur C Clarke*

3 DIGITAL IMAGE PROCESSING

An image can be defined as a two dimensional function, $f(x, y)$, where x and y are spatial coordinates of an image, and f can be a vector that represents the coordinates (x, y); referred to as the intensity or grey level of the image at that point. When the coordinates (x, y) and the intensity f are all finite discrete quantities, then the image is known as a digital image. Digital Image Processing (DIP) is a field, where an image is processed by means of a digital computer.

3.1 HISTORY OF DIGITAL IMAGE PROCESSING

The digital image was first used in the newspaper industry, the first pictures were sent by underwater cable, between London and New York. The introduction of Bartlane cables in the early 1920's, made it possible to transmit pictures across the Atlantic in less than three hours; which would otherwise take more than a week. For cable transmission a specialised printer: Halftone pattern printer was used to code the picture, which was then sent over the cable. This coded information was reconstructed at the receiving end (Gonzales et al, 2008). The printing method used in this procedure was abandoned in the early 1920's, because the printer was unable to distribute the intensity level properly. Therefore new photographic printers were installed at the receiving terminal which improved both the resolution and quality of the image. The Bartlane system used in 1921 was capable of coding an image up to 5 distinct grey levels; this was increased to 15 levels in 1929.

Though these digital images were used from 1920 to 1929, they did not involve any image processing techniques (Gonzales et al, 2008). The authors claim that to understand image processing one has to understand how computers evolved.

The modern digital computer was invented by John Von Neumann in the year 1940 with two important concepts first; a memory to store the program and data, and

second, conditional branching. These two ideas led to the development of CPU (Central Processing Unit) which is regarded as the heart of the computer. In 1960s computers were powerful enough to perform digital image processing. This was carried out at the Jet Propulsion Laboratory in Massachusetts Institute of Technology and at Bell Laboratories in the University of Maryland-most professionals consider this to be the birth of image processing. The cost was still fairly high for the computation at that era; however that changed in the 1970s, as dedicated hardware became available to perform image processing to meet the increased demand in digital image processing. In the mid-1980s there were numerous models of image processing which were sold as peripheral devices. In the early 1990s hardware was integrated inside a personal computer. As computers became more advanced and faster, they took over the role of hardware and more specialised software was created which can perform similar tasks. Companies such as MathWorks™ developed software specifically for image processing. This software for image processing consists of specialised modules or algorithms that can perform a specific task. A well-designed package allows the user to write minimum code, utilising the inbuilt algorithm to perform a desired function.

3.2 FUNDAMENTALS OF DIGITAL IMAGE PROCESSING

- Image acquisition: in this stage the scene whose image is required will be illuminated. The light reflected from the scene is captured through an image system-providing an analog image of the scene. This image will be sampled and quantized to form a digital image.
- Image enhancement: it is the manipulation of the original image, so that the image can be suitable for specific application. Enhancement techniques differ for different applications. There are no general guidelines for image enhancement; it all depends on the user which enhancement technique is best suited for an application.

- Image restoration: it deals with removing noise or other corruptions in the image so that the appearance of the image is improved. This is different form image enhancement. Image restoration is more objective and image enhancement is more subjective.
- Morphological processing: in this technique, a part of an image is extracted, that is used for describing the shape or representation of an image.

3.3 MATHEMATICAL MODEL OF A DIGITAL IMAGE

An image is always formed as a function of two components: first, illumination and second reflectance. The pixels present in the image or the value of this function is always non-negative and scalar, i.e. a positive integer. This function f can be mathematically expressed as

$$f(x, y) = i(x, y)\, r(x, y) \tag{3.1}$$

where, $i(x, y)$ is the illumination at the point (x, y); $0 \leq i(x, y) \leq \infty$, and $r(x, y)$ refers to reflectance at the point (x, y) with the limit $0 \leq r(x, y) \leq 1$. Here '0' indicates total absorption and '1' indicates total reflectance. The image captured is required to be converted into digital form by performing sampling and quantization.

3.3.1 Sampling

An image can be considered as a 2-D analog signal, defined as a signal which consist of continuous change in the light intensity along x and y axis. It consists of an infinite number of samples along both axes, and each sample can have a value from zero to infinity. To convert the analog image into digital form, the image must first be sampled along the x direction and sampled again along the y direction, and the number of samples considered, will affect the to the quality of the image. Let M and N be the number of samples taken along the x and y axes respectively, then the size of the image is $M \times N$.

3.3.2 Quantization

Quantization is the process of mapping an infinite number of sample values into a finite number of quantization levels. The number of quantization levels or step levels will in turn decide the number of bits required for each sample. If *L* represents the number of quantization levels, the number of bits per sample can be calculated from eq. (3.2):

$$L=2^k \tag{3.2}$$

where, *k* is the number of bits per sample, and the pixel can take the value '0' or '1'. This image is knows as a binary image. The pixel with the value '0' represents dark area and the pixel with the value '1' represents the bright area, hence the image consists of only two shades. If the quantization levels are more than 2, then the image is called a grey scale image, where the pixel value is always in the range between $0 \leq l \leq 1$, where *l* is the initial value of the pixel.

"Of all of our inventions for mass communication,
pictures still speak the most universally understood language"

- *Walt Disney*

4 IMAGE PROCESSING FOR VISUAL DEGRADATION

Peli was the first to introduce the concept of using digital image processing to enhance the image presented to patients suffering from visual degradation (Peli et al, 1984). To model a person's visual loss, a Contrast Sensitivity Function (CSF) was used, which was the inverse of the contrast threshold curve that represented the minimum contrast, or amplitude, necessary for a person to resolve whether sinusoidal intensity grating at various frequencies were horizontally or vertically oriented. They measured the CSF in various patients and used it to calculate individual visual degradation transfer functions (VDTF), which were the ratio of the CSF of the patients with cataracts to the CSF of persons with normal vision. Peli decided that using the VDTF as an inverse filter produced too much salt and pepper noise due to the amplification of the higher frequencies attenuated by a degraded visual system. He instead conjectured that adaptive image enhancement (Peli et al, 1982) may be better for enhancement. Although no testing was done in 1984 to see the effect of these enhancements on patients, the effect of inverse filter enhancement as viewed through simulated cataract conditions were studied. Additionally he addressed: contrast manipulation, spatial filtering, and pseudo colour recoding (Peli et al, 1991) attempts to improve reading rates in the visually impaired. Peli once again tackled enhancement using a pre-emphasis filter concept on limitations of image enhancement (Gonzales et al, 2008).

4.1 SPATIAL FILTERING

Image enhancement by spatial filtering would optimally amplify those spatial frequencies most attenuated by the visual system of the afflicted patients. Peli was investigating the use of the VDFT in an inverse filter enhancement technique (Peli et al, 1991). He mentioned a number of enhancements which would boost the high-frequency information in an image. High-pass image filtering techniques included:

un-sharp masking, extremum sharpening and adaptive filtering. Un-sharp marking subtracted a low-pass version from the original version. Extremum sharpening passed a spatial mask over the original image; the points inside this mask were assigned the maximum or minimum pixel value in the window, depending on which value the current pixel was closest to.

4.2 ADAPTIVE ENCHANCEMENT

Adaptive image enhancement involves low-pass filtering of the original image, and subtracting this low-pass filtered image from the original image, and adding this new image (which contained high-frequency information) to the original. Adaptive filtering was the same as adaptive image enhancement (Peli et al, 1982).

Peli tested adaptive image enhancement and adaptive thresholding in 1991 on patients suffering from low vision (Peli et al, 1991). He used Parametric Estimation by Sequential Testing (PEST) to minimize the number of measurements necessary to determine each patient's CSF. These enhancement techniques were not turned for a specific patient's CSF, but were turned to enhance the frequencies above 4 cycles per image which were most useful for face recognition. The results of the testing indicated that 39 out of 46 patient's tested had better facial recognition ability when viewing the enhanced faces than when viewing the un-enhanced faces.

4.3 WAVELETS

The previously-mentioned enhancement techniques represented a large and useful arsenal in the fight to restore recognition abilities in those with visually impairment. The most promising of the above rely on direct manipulation of an image's spatial frequency spectrum. The significance of discrete wavelet analysis compared to discrete Fourier analysis lies in the decomposition and reconstruction process inherent to wavelet analysis (Cohen & Ingrid, 1993). Here, it is seen that discrete wavelet analysis can be used as a tool for image enhancement and for simulating human perception of an image using a particular contrast sensitivity function. In his paper on contrast complex images, Peli mentioned image analysis and synthesis schemes using his log cosine implementation to determine band-limited contrast (Peli et al, 1991). One analysis scheme that has not been used, one that may more

closely represent visual processing, is wavelet analysis. Discrete wavelet co-efficient sets can be thought of as images that have been filtered in the frequency domain with filters having cut-offs at powers of two and bandwidths of one octave.

To decompose an image using the standard Discrete Wavelet Transform (DWT), two one-dimensional vectors are necessary: a vector representing the scaling function and a vector representing the wavelet function. The vector representing the scaling function is usually denoted as *h* and has a frequency response displaying low –pass characteristics. The vector representing the wavelet function is usually denoted as *g* and has a frequency response displaying high-pass characteristics. *h* and *g* form an orthogonal basis set (Olivier et al, 1991).

With simple orthogonal wavelets, a single vector is given for the scaling function. The wavelet co-efficient vector is generated from the scaling coefficient using the relationship,

$$g(n) = -1^{1-n} \times h(1 - n) \tag{4.1}$$

Now, that these two vectors are available, the actual image decomposition is accomplished by using the mirrors of these two vectors; that is $\bar{h}(x) = h(-x)$ and $\bar{g}(x) = g(-x)$ are the vectors that are actually used in the decomposition operation.

"We're changing the world with Technology."

- *Bill Gates*

5 METHODS

Two possible methods are described in this chapter that could be used to design a computer display for individuals with a low-order visual impairment.

5.1 GEOMETRICAL OPTICS METHOD

Geometrical optics describes the propagation of light as it travels from one medium to another. Light rays travel along a straight line in a homogeneous medium; the rays of light can be reflected, refracted or absorbed depending on the surface. Geometrical optics is the best approximation that shows the behaviour of the light, which can be used to describe an image. To decrease complexity in the geometry, one can use paraxial approximation-then the mathematical model becomes linear; hence optical elements can be described by simple matrices. This matrix can be used for many applications (Nussbaum et al, 1976).

5.1.1 Refraction

When a ray of light is incident on the interface separating two different media characterised by n_1 and n_2, as shown in figure 5-1, it is well known that part of the light is reflected back into the first medium, while the rest of the light is refracted as it enters the second medium. The direction taken by this ray of light is described by the laws of reflection and refraction, which can be derived from Fermat's principle.

Consider a light ray traveling from point A to point B with two different density of medium shown in figure 5-1, as the light ray travels from A to B; at the interface between these medium, the light get refracted or bent, the degree of refracted ray is stated in Snell's law.

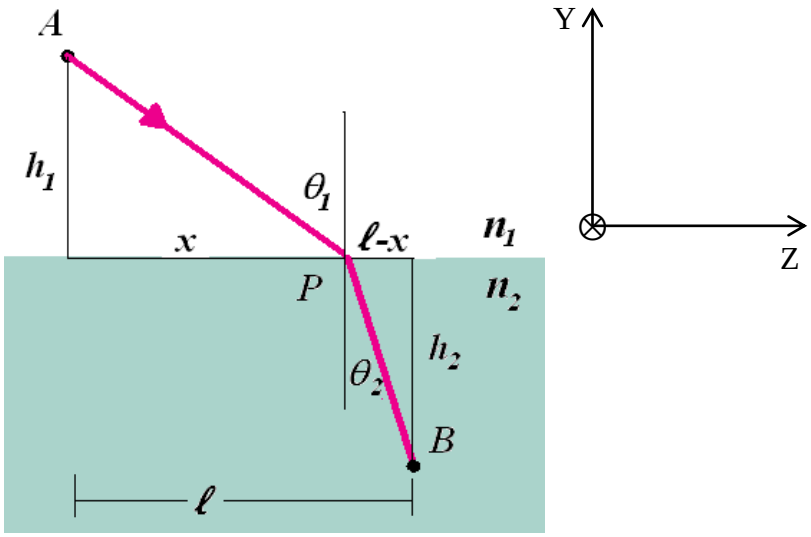

Figure 5-1 Refraction of light as it travel from one medium to another (Fermat & Wei, 2009).

5.1.2 Ray Transfer Matrix

Matrices can be used to describe ray propagation through an optical system. To derive a refraction matrix a spherical optical system is considered, where all the points comprising to the succession of spherical refractive surface are all centred on the same axis called the optical axis. Let the optical axis be long the *z*-axis and consider all the rays that lie in *xz* plane and those that are close to the *z*-axis. These rays are called paraxial rays. They lie very close to the optical axis, so that their angle of deviation is very small form the optical axis. Therefore $tan\ \theta \approx sin\ \theta \approx \theta$. This is because all paraxial rays will intersect at a point after travelling through an optical system.

Now, let us consider the propagation of a paraxial ray through the optical system shown in figure 5-2. A ray that is incident on the first surface can be expressed by its height x_1 from the optical axis and by its angle θ_1 made at the plane. In figure 5-2, the quantities (x_1, v_1) give the coordinates of the incident ray in the *z*-plane. This angle θ of the incident ray can be replaced by $v = n \times \theta$, where n is the refractive index of the medium. From figure 5-2, the ray of light will pass through the input plane with (x_1, $v_1 = n_1\ \theta_1$) as coordinates and into the optical system and finally exit at the output

plane with (x_2, $v_2 = n_2$, θ_2) as output coordinates. Since it is considered as a paraxial approximation, the output variables linearly depend on the input values. The transformation from input to output is represented in matrix form using eq. (5.1).

$$\begin{bmatrix} x_2 \\ v_2 \end{bmatrix} = \begin{bmatrix} \mathbf{A} & \mathbf{B} \\ \mathbf{C} & \mathbf{D} \end{bmatrix} \times \begin{bmatrix} x_1 \\ v_1 \end{bmatrix} \tag{5.1}$$

Here, the elements **ABCD** is called the ray transfer matrix.

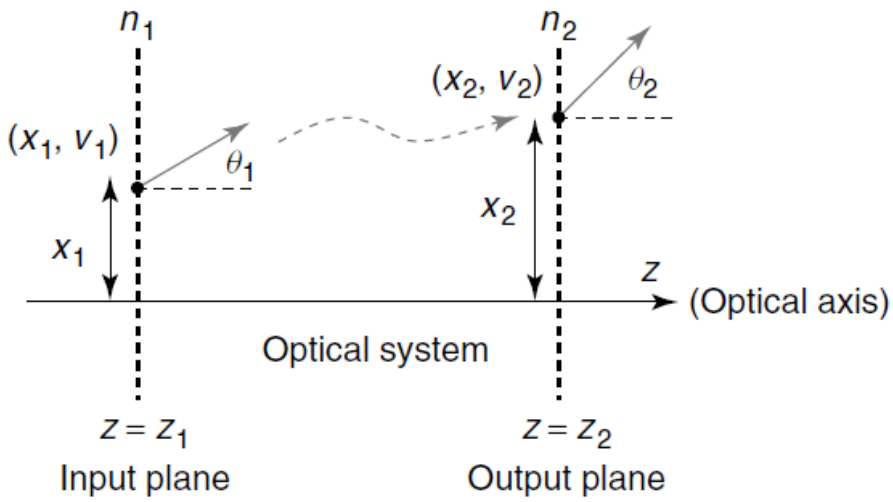

Figure 5-2 Input and output plane in an optical system (Poon & Liu, 2011).

5.1.3 Thin-Lens Matrix

Consider the thin lens shown in figure 5-3. As shown in the figure, (x_1, v_1) is the input ray coordinate and (x_2, v_2) is the output ray coordinate that are linked by the three matrices; a refraction matrix at surface one, followed by a translation matrix in the lens, and another refraction matrix at surface two described by eq. (5.2):

$$\mathbf{S} = \mathbf{R_2 T_d R_1} \tag{5.2}$$

Eq. (5.2) can be re-written as:

$$\begin{bmatrix} x_2 \\ v_2 \end{bmatrix} = \mathbf{S} \begin{bmatrix} x_1 \\ v_1 \end{bmatrix} \tag{5.3}$$

Here, **S** is called as the system matrix.

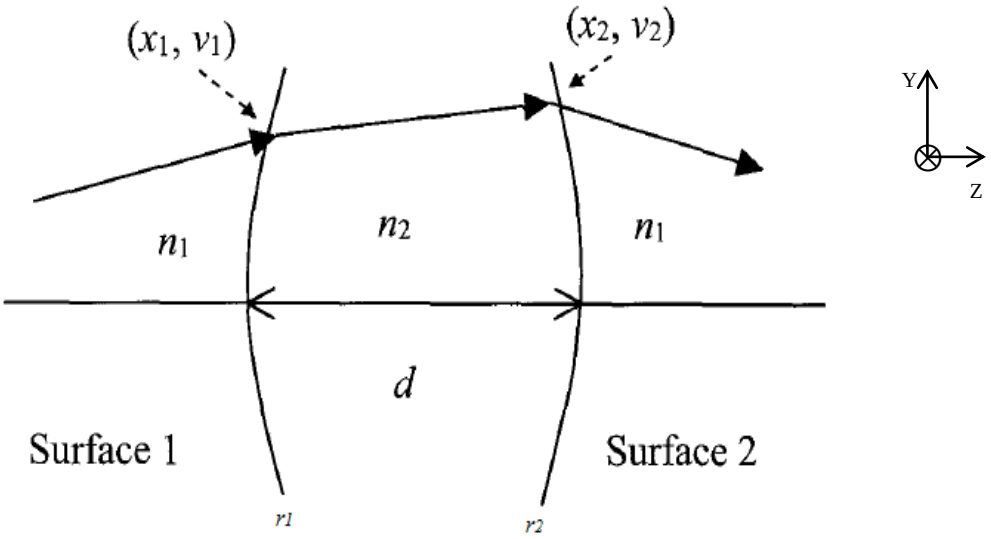

Figure 5-3 A thin lens; with thickness *d*, radii of curvature r_1 and r_2 at surfaces 1 and 2 respectively (Poon et al, 2006).

To determine the coefficients of the refraction matrix $\mathbf{R_1}$ and $\mathbf{R_2}$, consider a spherical surface that separates two regions of refractive indices n_1 and n_2 as shown in figure 5-4, with C as the centre of the curved surface and *r*, the radius of curvature. The ray of light strikes at the point A on surface one, at an angle ϕ_i, this is known as the angle of incidence and gets refracted at an angle ϕ_t, called the angle of refraction. In figure 5-4, *x* denotes the height from the optical axis to the point A where the light strikes the first surface. Then the angle ϕ which is subtended at the centre C becomes:

$$sin\, \emptyset \approx \frac{x}{r} \approx \emptyset \tag{5.4}$$

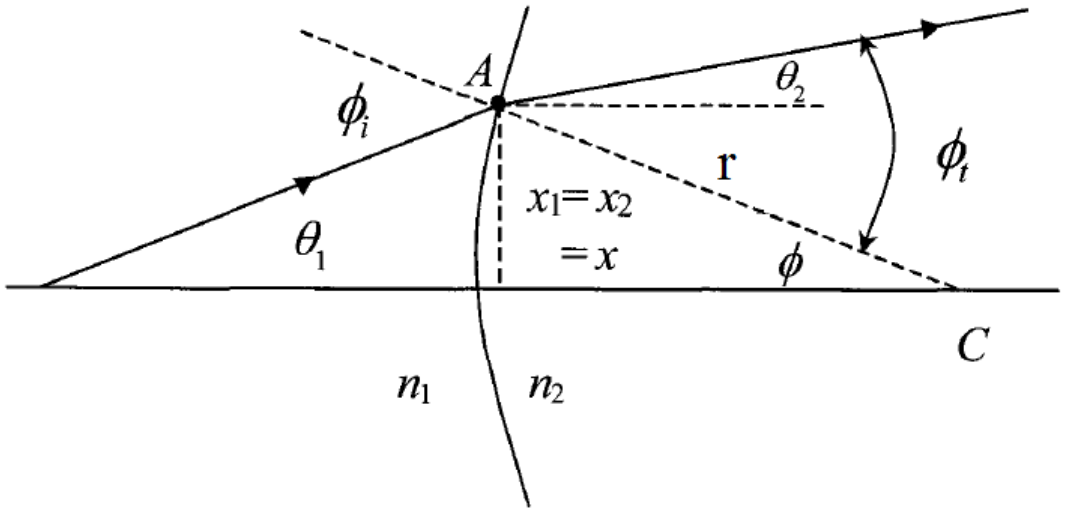

Figure 5-4 Ray of light incident on a curved surface gets refracted, obeying Snell's law (Poon et al, 2006).

From figure 5-4 it can be noted that the height of the ray at point A, before and after refraction is the same i.e. $x_1 = x_2$, therefore v_2 can be expressed in terms of x_1 and v_1. Applying Snell's law and using the paraxial approximation,

$$n_1 \phi_i = n_2 \phi_t \tag{5.5}$$

using basic geometry and from figure 5-4,

$$\phi_i = \theta_1 + \phi \quad \& \quad \phi_t = \theta_2 + \phi \tag{5.6}$$

from eqs. (5.5) and (5.6),

$$n_1 \phi_i = v_1 + \frac{n_1 x_1}{r} \tag{5.7}$$

$$n_2 \phi_t = v_2 + \frac{n_2 x_2}{r} \tag{5.8}$$

Using eqs. (5.5), (5.7) and (5.8) and the condition $x_1 = x_2$:

$$v_2 = \frac{n_1 - n_2}{r} x_1 + v_1 \tag{5.9}$$

Hence, the refraction matrix, relating all the coordinates of the ray before and after refraction:

$$\begin{bmatrix} x_2 \\ v_2 \end{bmatrix} = \begin{bmatrix} 1 & 0 \\ -p & 1 \end{bmatrix} \begin{bmatrix} x_1 \\ v_1 \end{bmatrix} \tag{5.10a}$$

Where the coefficient p is:

$$p = \frac{n_2 - n_1}{r} \tag{5.10b}$$

The eqn. (5.10a) is called the refractive matrix of the spherical surface, and r is the radius of curvature, measured in meters, then the quantity of p is measured in dioptres. For a convex lens the power is taken as positive and negative for the concave lens. The refractive matrix **R** is a (2×2) transfer matrix, that describes the refraction of the light when it touches a spherical surface, shown in eq. (5.11).

$$\mathbf{R} = \begin{bmatrix} 1 & 0 \\ n_2 - n_1/r & 1 \end{bmatrix} \tag{5.11}$$

Now, this refracted ray will travel in the lens medium with the velocity c/n_2; the translation matrix will describe the ray travelling through this homogeneous medium, with refractive index n_2 converging a distance d. since it is an homogeneous medium, the ray travels in a straight line represented in the figure 5-5.

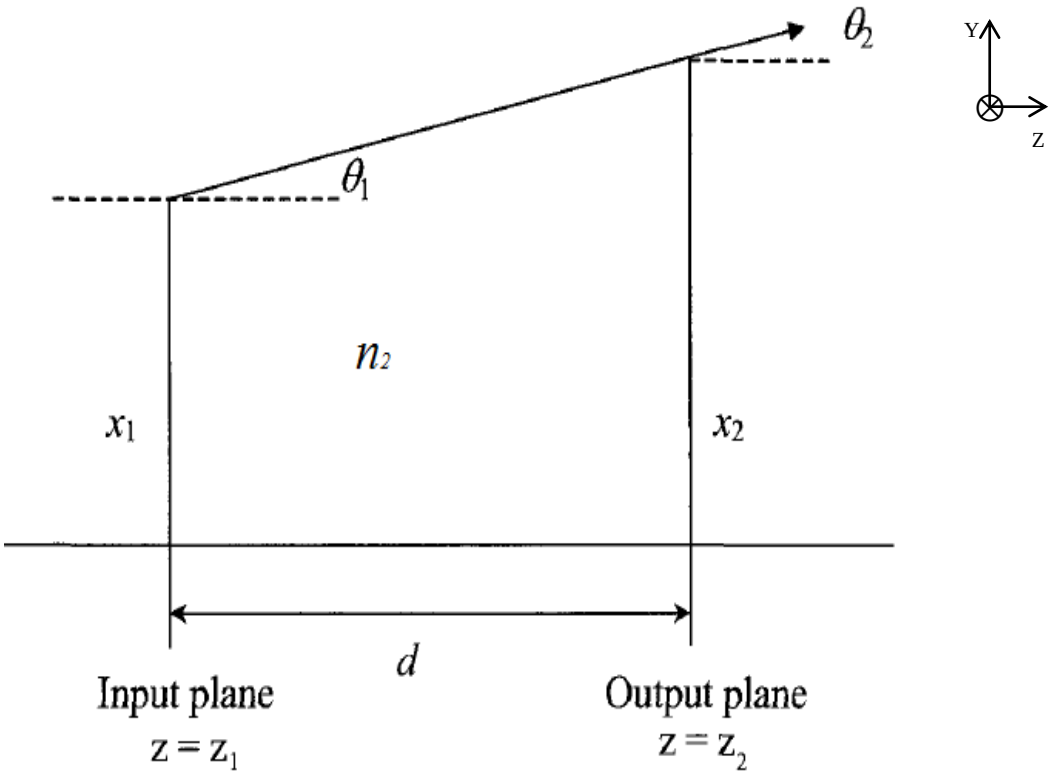

Figure 5-5 Propagation of light through a lens with refractive index n_2 (Poon et al, 2006).

The general equation of a straight line is written as:

$$y = mx + c \tag{5.12}$$

here, m is the slope of the straight line and c is a constant. From eq. (5.12) and light since travels in a straight line, the distance travelled by the light is given as:

$$x_2 = x_1 + d \tan \theta_1 \tag{5.13}$$

and

$$n\theta_2 = n\theta_1 \quad \text{or} \quad v_2 = v_1 \tag{5.14}$$

From eqs. (5.13) and (5.14), the output and the input coordinates of the ray can be related to form a transformation matrix:

$$\begin{bmatrix} x_2 \\ v_2 \end{bmatrix} = \begin{bmatrix} 1 & d/n_2 \\ 0 & 1 \end{bmatrix} \begin{bmatrix} x_1 \\ v_1 \end{bmatrix} \tag{5.15}$$

Therefore;

$$\mathbf{T}_d = \begin{bmatrix} 1 & d/n_2 \\ 0 & 1 \end{bmatrix} \tag{5.16}$$

The eq. (5.16) is a (2 × 2) translation matrix of the ray-travelled through a distance *d* in a homogeneous optical system with the refractive index n_2.

Substituting eqs. (5.11) and (5.16) in eq. (5.2), the system matrix can be re-written as,

$$\mathbf{S} = \begin{bmatrix} 1 & 0 \\ n_2 - n_1/r & 1 \end{bmatrix} \begin{bmatrix} 1 & d/n_2 \\ 0 & 1 \end{bmatrix} \begin{bmatrix} 1 & 0 \\ n_1 - n_2/r & 1 \end{bmatrix} \tag{5.17}$$

In the above eq. (5.17), n_1 and n_2 are interchanged in the refractive matrix $\mathbf{R_2}$, because at the second surface the light rays travel from denser to rarer medium with the refractive index n_2 and n_1 respectively.

5.2 FOURIER OPTICS METHOD

A new algorithm was developed by using the wavefront aberration of the users' eye. This is a new approach to facilitate computer access to a person with low visual impairment. There are few algorithms developed in the past, one which is very similar to the lens that uses a spatial light modulator hence providing a clean image to the user (Liang et al, 1997) this particular model is very complicated, bulky and it require many supporting components. Jiang in the year 1990's came up with a very ingenious way to transform the image using an deformable mirror and he measured the aberration of the eye online (Thibos et al, 1990). Through this was very effective, had few drawbacks as the user always had to connect to the network when he wished to use his computer display, hence this model was not effective and user friendly.

A simple and effective way is to transform the image at its source, image processing techniques could be applied to the image before it presented to the user-based on the person's wavefront aberration function. The idea of pre-compensation is to alter the image in such a way that it reverses the effect of the wavefront aberration of the eye. After this, the modified image is displayed to the user, the wavefront aberration of the observer and the pre-compensation image will cancel out each, resulting in an image that could be perceived by a visual impairment person. Hence it does not require any additional equipment's. Each user's visual aberration much be known to generate the visual information that is unique to the user, therefore this provide personalised display that could run on a normal personal computer (Jr & Barreto, 2004).

5.2.1 Human Eye as an LTI system

An optical system can be considered as a Linear Time Invariant (LTI) system (Goodman, 1996), thus, all the properties of a conventional LTI will also hold good for an optical system. Let the image formed on the retina be $R(x, y)$, this image is obtained by the convolution of the system input $I(x, y)$ with the Point Spread Function (PSF) $H(x, y)$:

$$R(x, y) = I(x, y) * H(x, y) \tag{5.18}$$

In eq. (5.18), '*' denotes the convolution operator. The blurring of the image occurs in the eye because the lens in the eyes project the light from the object to different points in the retina, rather than projecting it to a single point, this leads to a broad Point Spread Function (PSF) in the eye.

The real world image $I(x, y)$ are stored in a computer as a digital image, that will be viewed by the user in an computer display screen, this digital image is represented as $DI(x, y)$. Now the retinal image $R(x, y)$ is formed by the convolution of the digital image with the PSF of the observer's eye, shown in eq. (5.19):

$$R(x, y) = DI(x, y) * H(x, y) \tag{5.19}$$

The image that should be displayed to the user, $UD\ (x, y)$ can be obtained from convulsing the digital stored image in the computer $DI\ (x, y)$ with the inverse PSF of the user's eye $H^{-1}\ (x, y)$, in eq. (5.20),

$$UD\ (x, y) = DI\ (x, y) * H^{-1}\ (x, y) \tag{5.20}$$

From eq. (5.19) and (5.20), the retinal image seen by the viewer can be stated in eq. (5.21):

$$R\ (x, y) = \{DI\ (x, y) * H^{-1}\ (x, y)\} * H\ (x, y) \tag{5.21}$$

From eq. (5.21) one can predict that $R\ (x, y)$ is an image that a user would perceive by seeing the digital stored image $DI\ (x, y)$. This equation is a result of deconvoluting-the displayed image with the inverse PSF. Hence by using a deconvolution procedure a blurred image can be restored to obtain a modified image. If deconvolution is applied to a clear image then it produces a pre-compensated image. When this image is viewed on a computer display by the user with low or high visual impairment, it projects a clear image on the retina. Thus, deconvolution steps can be practically implemented with good results (Alonso et al, 2004, Gonzales et al, 2008).

5.2.2 Practical Method

The PSF of the eye can be found using the Hartmann-Shack principle which is a wavefront analyser. A wavefront is a physical representation of the quality of light beam refracted from an optical system. The quality of the light can be distorted by an optical system such as lens. In a normal eye plane rays converge to form a clear image on the retina but if these plane rays are falsely bent by the lens then they produce disrupted image.

The wavefront is measured by a device called aberrometer; it measures the aberration, hence the name wavefront aberration. An aberration is a visual defect of the eye and occurs when the ray of light is incorrectly refracted; it can be due to a defect in the shape of the eye. Myopia and hyperopia are considered as low order aberrations and spherical aberration is more serious. Statistics show that 90% of

visually impaired persons fall under the category low-order aberration. The aberrometer uses a wavefront that measures the total refractive power of the eye. This is done by plotting how a ray of light travels through the eye.

Ophthalmologists claim that in recent year's wavefront aberration enables them to measure the total refractive error of an eye, including myopia, hyperopia, astigmatism and other more complex refractive errors that could be corrected with conventional glasses. Shack Hartmann based measuring devices are quicker and more accurate when compared to other conventional measuring devices, and calculates the aberration in one shot, since the longer the time taken by the device, the more negative effects on the eye (Alonso et al, 2004).

The pupil function $P(x, y)$ could be considered as a wavefront aberration function $W(x, y)$. the pupil function describes all the imaging properties of an optical system- here the pupil function refers to the pupil of the eye (Williams et al, 2002). This function is given as,

$$P(x, y) = A(x, y) e^{\frac{-j 2 \pi n W(x, y)}{\lambda}} \tag{5.22}$$

Here $A(x, y)$ is the amplitude of the light that pass through the pupil, for simplicity it can be taken as 1, n is the refractive index of the eye and λ is the wavelength of the light in vacuum (Jr et al, 2004, Salmon, 1999).

Using Fourier Optics, one could derive an Optical Transfer Function (OTF) for a specific use (Williams et al, 2002), therefore an OTF is for this purpose is obtained by convoluting the pupil function $P(x, y)$ with its complex conjugate (Williams et al, 2002, Wilson, 2001) shown in the eq. (5.23),

$$O_T(x, y) = P(x, y) * \overline{P(-x, -y)} \tag{5.23}$$

Optical Transfer Function and Fourier transform pair can be written as in the eq. (5.24).

$$O_T(x, y) = F\{H(fx, fy)\} \tag{5.24}$$

The PSF of the user's eye could be found out by the above mentioned procedure and this can be used in deconvolution process. To implement deconvolution, inverse filtering technique can be used, many text have shown that inverse filtering could be used in image processing application to restore a blurred image with a known blurring function (MathWorks, 2001).

The input and the output of any linear system can be related with a convolution operator stated in eq. (5.25),

$$X(x, y) = Y(x, y) * H(x, y) \tag{5.25}$$

In this equation, $X(x, y)$ is the image that must be presented to the observer, $Y(x, y)$ is the blurred image and $H(x, y)$ is the known blurring function. Using the Fourier transform property of convolution, the degraded or blurred image could be found using eq. (5.26),

$$Y(x, y) = F^{-1}\left\{\frac{F\{X(x, y)\}}{F\{H(x, y)\}}\right\} \tag{5.26}$$

where $F\{X(x, y)\}$ and $F\{H(x, y)\}$ are the Fourier Transforms of $X(x, y)$ and $H(x, y)$, respectively.

Using eq. (5.26), the image formed on the retina $RD(x, y)$ can be found,

$$RD(x, y) = F^{-1}\left\{\frac{F\{DI(x, y)\}}{F\{H(x, y)\}}\right\} \tag{5.27}$$

Here the main objective is to deconvolve the stored digital image $DI(x, y)$ along with the PSF of the observer's eye $H(x, y)$. This equation is known as the Optical Transfer Function of the user.

Numerous text and journal articles have shown the implementation of inverse filters using optical transfer functions, however these filters possess many limitations. One

method presented by Alonso is the use of Minimum Mean Square Error or the Weiner filter (Gonzales et al, 2004), hence eq. (5.27) becomes:

$$RD\,(fx, fy) = \left[\frac{1}{H(fx, fy)} \times \frac{|H(fx, fy)|^2}{|H(fx, fy)|^2 + K}\right] \times I\,(fx, fy) \tag{5.28}$$

In the eq. (5.28), $I\,(fx, fy), H(fx, fy)$ and $RD\,(fx, fy)$ are the Fourier transforms of $I\,(x, y)$, $H\,(x, y)$ and $RD\,(x, y)$, respectively.

"It is appallingly obvious our technology has exceeded our humanity."

- *Albert Einstein*

6 IMPLEMENTATION

Two different algorithms are written in Matlab®, one using geometric optics and another using a Fourier optics method. The design steps are discussed in this chapter.

6.1 ALGORITHM I USING GEOMETRIC OPTICS

Form eq. (5.17), which gives the system transfer matrix of an optical system, the behaviour of light is described as it travels through the lens. This transfer function matrix was implemented in Matlab® and the matrix coefficients were taken as follows: refractive index of lens was assumed to be 1.489 ("Lenses and Lens Options", 2005) which is the refractive index of a plastic lens; plastic lens are usually preferred then crown or glass lens because plastic lens are light and hard when compared to conventional crown lens, more UV resistance then glass lens. ("Ophthalmic Products," 2012, "Refractive Source," 2012) hence in the implementation of the algorithm plastic lens is considered. A Plano-concave lens with -2 dioptre and 168.75mm as the radius of curvature is considered. This calculated using eq. (6.1) ("Diopter conversion chart", 2012)

$$radius\ of\ curvature = \frac{337.5}{diopter} \tag{6.1}$$

The radius of curvature on the plane surface of the lens is infinity, therefore for the purpose of calculation a large value i.e. 10^6m is considered as a radius of curvature at the plane surface. All these values were tabulated to the appropriate coefficients of the matrix.

The translation matrix, which represents the propagation of light inside an optical system, was evaluated. The thickness of the lens *d* was found out by using eq. (6.2), i.e., $3.607 \times 10^{-3}m$. The ray track path was found by using the eq. (5.17), and matrix coefficient was evaluated.

$$thickness = \left(\frac{(0.5 \times diameter)^2 \times lens\ power}{(2000 \times (refractive\ index\text{-}1))} \right) \quad (6.2)$$

All the values of three matrixes were multiplied; since the number of rows and columns are the same, a system matrix that describes the light path in an optical system was obtained. This system matrix was used as filter coefficients to transform an image that can be viewed by a visually impaired person.

6.1.1 Results and Discussion

A JPEG colour image of Lena with dimensions 256 × 256 was read into a Matlab® m-file and converted into the grey image shown in figure 6.1. This image was filtered using the filter coefficients described in the transfer matrix and the resultant image is shown in figure 6-2.

As shown in the figures, these are not the actual results expected; the expected result was a filtered image that could be seen by a refractive error user. A histogram is shown in figure 6-3, a better understanding of an image can be inferred, histogram on the left hand side shows the pixel distribution of a the original image, the histogram suggests that there are no pixels below the grey intensity level 25 and above 225. It can also be seen that most of the pixels are at the centre of the graph indicating an even distribution of grey scale. On the right is the histogram of the filtered image, the first notable element is that all pixels have moved to the right side of the graph and certain pixels have reached their highest brightness, this can also be seen in the picture, as it has turned bright.

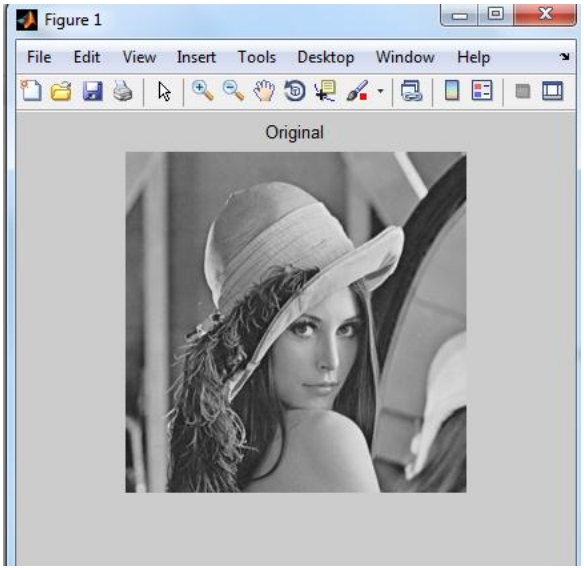

Figure 6-1 Original Lena image.

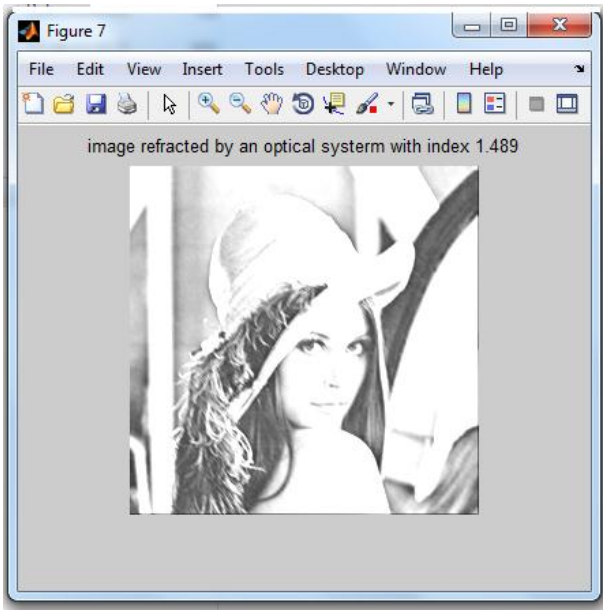

Figure 6-2 Image obtained after filtering with a transfer matrix.

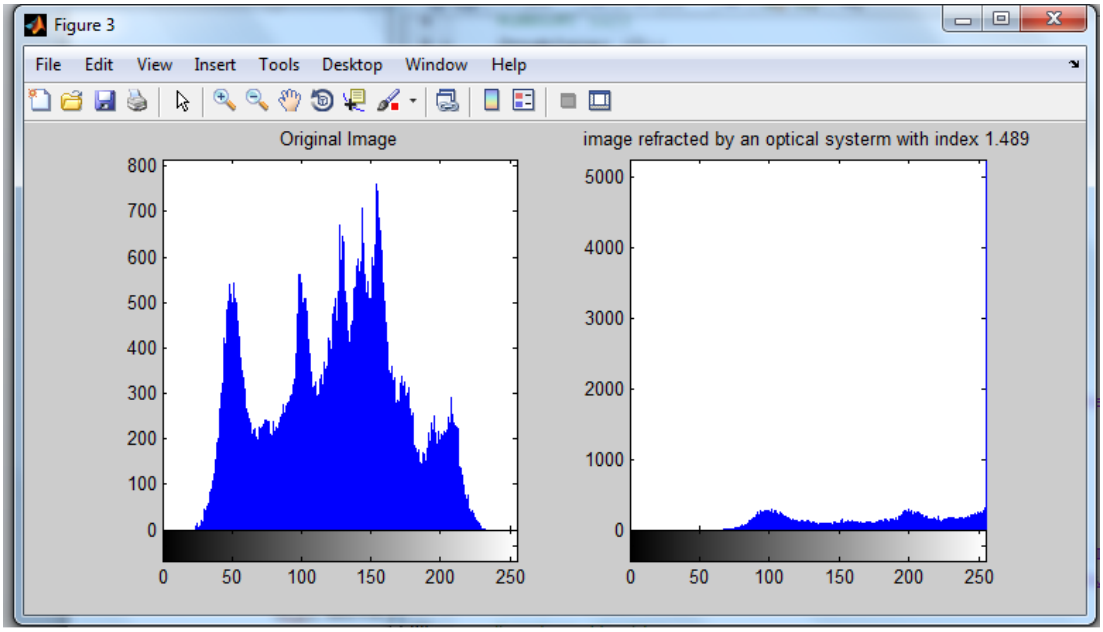

Figure 6-3 Histograms of the original image on the left and filtered image on the right.

6.2 ALGORITHM II USING FOURIER OPTICS

To design an algorithm using Fourier optics method, one must know the users' Point Spread Function; this can be calculated from eq. (5.22). This function could be used to blur the image as stated and shown by Alonso (Jr & Barreto, 2003).

6.2.1 Results and Discussion

The PSF is evaluated by taking the user's pupil diameter and the wavelength of the light. A pupil diameter of 6.32mm was considered for this experiment. Experimental results by Neil (2009) show that most of the myopic subjects with -2 to -6 dioptre lens have a pupil diameter of 5.48 ± 0.84. For this experiment maximum pupil aperture is preferred (Charman & Radhakrishnan, 2009). The light wavelength of 560nm is preferred, because studies have showed that human eye is more sensitive to yellow-green light with frequency 1.785 kHz (Zhao, 2007). The PSF was calculated using eq. (5.22) with all the above parameters; the PSF is shown in figure 6-4.

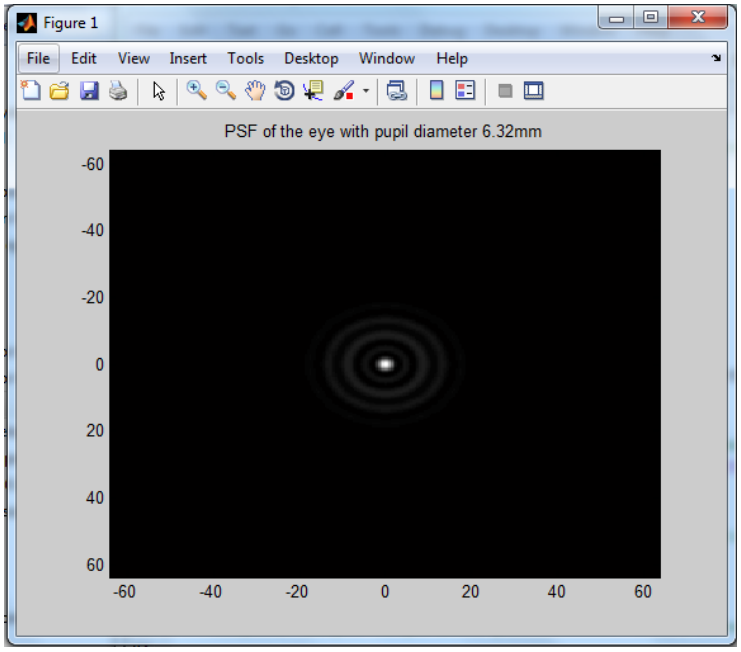

Figure 6-4 PSF of the eye with pupil diameter 6.32 mm.

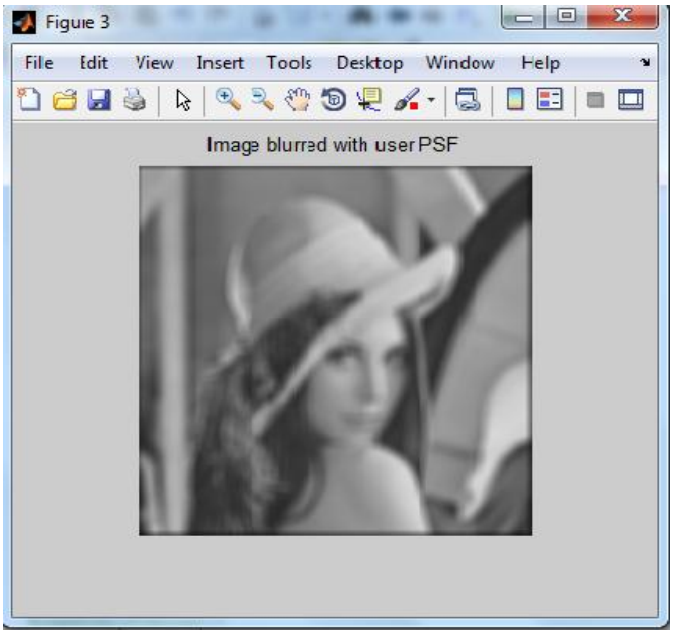

Figure 6-5 Blurred image using wavefront aberration of the user.

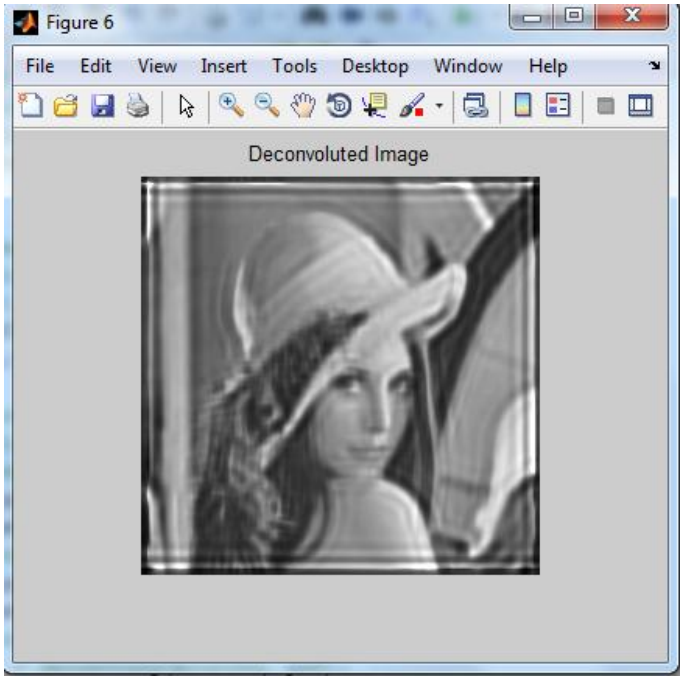

Figure 6-6 After the deconvolution process.

A 256 × 256 digital colour image of Lena was read into the Matlab script, and converted into a grey scale image for simplicity, shown in figure 6-1. This grey image was then blurred with the user's PSF; the result of this blur is figure 6-5. Figure 6-6 shows the result of deconvolution, which was obtained from figure 6-5, as it was deconvoluted using the PSF of the eye.

The deconvolved image is not the exact replica of the original image, but it is a transformed image that can be seen by a myopic user without the need of corrective lens.

The algorithm is not restricted only for myopia; it can be used for hyperopia and also to certain degree astigmatism. For the use of hyperopia and astigmatism the exact pupil aperture must be entered into the script, and it generates an image suitable for the user.

Since this code is written in a general format, subject testing was not possible, because every individual has a different wavefront aberration, hence an image transformed for one user may not be seen by another user. However, this algorithm was written for a pupil diameter of 6.32mm and any observer with that diameter could see the deconvolved image.

"My interest is in future because I am going to spend the rest of my life there"

- *Charles F. Kettering*

7 CONCLUSIONS AND FUTURE WORK

This thesis presented two possible methods that could be implemented to alter an image so that a visual impaired person could see the image without the need to wear spectacles.

The geometrical optic is considered as an old area of science, yet there are no reports of this method being implemented to modify an image preferable for a person with a refractive error. This thesis shows geometrical optics can be used to change an image suitable for myopic and hyperopic users. This may not be the best method for image modification, but this does not imply that geometric optics can never be used to alter an image.

Optics describes how a ray of light is reflected, refracted and diffracted; these are governed by mathematical equations. These equations hold good for a single ray of light. But while viewing an object at a distance; the object reflects the light from all its possible points, hence while considering a transfer matrix, all these light sources must be taken into account, but this leads to an infinite number of matrices making the computation very complex.

Thus, this area prospects a huge number of scientist and researchers. More research in this field could improve knowledge in this area, and broaden the application of geometric optics.

Fourier optics is a combined study of optics and Fourier transforms. There are numerous research papers on Fourier optics that are applied for image processing techniques, and quite a few on image processing for visual impairment.

Using Fourier optics, an image could be modified for a refractive error user, and one of the methods is to determine the spherical wavefront aberration in the eye and use this to generate a Point Spread Function (PSF). This PSF is used as an impulse response, and is convolved with the original image, resulting in a blurred image. The blurred image can then be deconvolved by the same PSF, hence the original image is altered for a visual disability user.

The results obtained from this method are satisfactory, because in deconvolution the image obtained may not be the required image for the user. The deconvolution also adds little noise to the new image and dis-alters the edges of the de-blurred image due to aliasing.

One method to reduce noise is to deconvolve the image multiple times, until the desired output is obtained. Instead of convolution and deconvolution, the image and the PSF of the eye are multiplied with their appropriate Fourier transform, which acts as a convolution process. The blurred image can be evaluated by taking inverse Fourier transforms. For deconvolution, the FT of both image and PSF are divided and the IFFT gives the de-blurred image for a visual impaired person.

One possible expansion of this field is to develop more robust algorithms that can modify the image exactly as the user prefers, this algorithm uses grey images, a more complex Matlab® scripts can be designed that can process colour images. Instead of a static code a new real time program can be invented, where the program processes the image in real time and totally eliminates the use of glasses for a lens corrected individual. Ophthalmology clinics could be installed with Shack Hartmann wave aberration measurement devices, the wave aberration function could be included in the prescription. The user could then enter his aberration function on the real time program and the computer will alter the image best focused for the user.

Another method is the use of Graphical User Interface (GUI). The algorithm must be able to alter the image or text automatically, i.e., when an image is presented on the screen, the user is provided with an option to degrade the image, which can be seen by the user without the need of glasses. The algorithm must also provide the degree of degradation in the image by providing the corrected lens power used by the user and the wave aberration in the eye of the user.

REFERENCES

Alonso, M., J. (2004). An Improved Method of Pre-Deblurring Digital Images Towards the Pre-Compensation of Refractive Errors. *SoutheastCon, 2005. Proceedings. IEEE* (pp. 421–427).

Ambrosio, R; Tervo, T; Wilson, S. (2008). LASIK-associated dry eye and neurotrophic epitheliopathy: pathophysiology and strategies for prevention and treatment. *Journal of Refractive Surgery*, *24*(4), 396–407.

Budowa. Retrieved from http://195.117.188.199/rozdzial_1_12.htm

Campbell, J. R. (2006). Marin Eyes. *Marin Ophthalmic Consultants*. Retrieved from http://www.marineyes.com/anatomy/anatomy.html

Charman, W. N., & Radhakrishnan, H. (2009). Accommodation, pupil diameter and myopia. *Ophthalmic & physiological optics : the journal of the British College of Ophthalmic Opticians (Optometrists)*, *29*(1), 72–9. doi:10.1111/j.1475-1313.2008.00611.x

Chuang, Eliseu Y; Li, De-Quan, Fang, X. (2008). Effects of Contact Lens Multipurpose Solutions on Human Corneal Epithelial Survival and Barrier Function. *Eye & Contact Lens: Science & Clinical Practice*, *34*(5). doi:10.1097/ICL.0b013e3181842518

Cohen, A., & & Ingrid, D. (1993). Wavelets on the Interval and Fast Wavelet Transforms. *Applied and Computational Harmonic Analysis*, *1*(1), 54–81.

Diopter conversion chart. (2012).*ArtOptics.com*. Retrieved from http://www.artoptical.com/files/documents/resources/Diopter_Conversion_Chart.pdf

Fermat, F., & We, A. (2009). Fermat ' s Principle and the Laws of Reflection and Refraction. *Physics 5B*, 1–2.

Generic Look.com. (2012).*Medical Encyclopedia*. Retrieved from http://genericlook.com/anatomy/Eyeball/

Gonzales, R.C; wood, R. E. (2008). *Digital Image Processing* (Third Edit.). New Delhi: Pearson Education, Inc.

Goodman, J. W. (1996). *Introduction to Fourier Optics* (second edi.). McGraw-Hill companies, INC.

James, G. P. (2010). Cataract and Laser Institute. *St Luke's*. Retrieved from http://www.stlukeseye.com/Conditions/cmv.html

Jr, M. A., & Barreto, A. (2003). An Image Processing Approach to Pre-compensation for Higher-Order Aberrations in the Eye F. *SYSTEMICS, CYBERNETICS AND INFORMATICS*, *2*(3), 1–4.

Jr, M. A., & Barreto, A. (2004). Image Pre-Compensation to Facilitate Computer Access for Users with Refractive Errors. *ASSETS*, 126–132.

Lenses and Lens Options. (2005).*Opticiansfriend.com*. Retrieved from http://www.opticiansfriend.com/lenses.html

Liang, J., Williams, D. R., & Miller, D. T. (1997). Supernormal vision and high-resolution retinal imaging through adaptive optics. *Journal of the Optical Society of America. A, Optics, image science, and vision*, *14*(11), 2884–92. Retrieved from http://www.ncbi.nlm.nih.gov/pubmed/9379246

Love, G. D. (2000). *Proceedings of the 2nd International Workshop on Adaptive Optics for Industry and Medicine* (First Edit., pp. 57–62). Singapore: World Scientific Publishing Co. Pte. Ltd.

Martini, Ferderic H; Nath, J. L. (2009). *Fundamentals of Anatomy & Physiology* (Eighth Edi.). San Francisco: Pearson Education Inc.

Mason, P. (2008). Neuroanthropology. Retrieved from http://neuroanthropology.net/2008/09/04/colour-is-it-in-the-brain/

MathWorks. (2001). *Image Processing Toolbox, User's Guide* (Version 3.). MathWorks, Inc.

McFadden, D. M. M. (2005). LASIK laser eye surgery. Retrieved from http://www.lasik1.com/medical.html

Mount Nittany Health. (2009).*Healthsheet*. Retrieved from http://www.mountnittany.org/articles/healthsheets/7224

New Contact Lens Fits Pupil Only. (1952, February 11).*The NewYork Times*. New York.

Nussbaum, Allen; Phillips, R. A. (1976). *Comtemporary Optics for Scientists and Engineers*. (N. Holonyak, Ed.) (First Edit.). New Jersey: Prentice Hall-Inc.

Olivier, Rioul; Vetterli, M. (1991). Wavelets and Signal Processing. *IEEE SPICE Magazine*, 14–38. doi:1053-5888/91/1000-0014

Ophthalmic Products. (2012).*Carl Zeiss Vision Inc*. Retrieved from http://www.zeiss.com/41256820002524A3/Contents-Frame/E83832252EC1FF4E852572250059E704

Peli, E.; Peli, T. (1984). Image Enhancement for the Visually Impaired. *Optical Engineering*, *23*(1), 47–51.

Peli, Eli ; Goldstein, Robert; Young, G. (1991). Image Enhancement for the Visually Impaired. *Investigative Ophthalmology & Visual Science*, *32*(8), 2337–2350.

Peli, T., Jae, S. L. (1982). Adaptive Filtering for Image Enhancement. *Optical Engineering*, *21*(1), 108–112.

Poon, T., & Liu, J. (2011). Fundamentals of Optics.

Poon, Ting-Chung; Kim, T. (2006). *Engineering Optic with Matlab* (First Edit.). Singapore: World Scientific Publishing Co. Pte. Ltd.

Refractive Source. (2012).*Access Media Group LLC*. Retrieved from http://www.refractivesource.com/patients/alternatives/glasses/lenses-material.htm

Salmon, T.(1999). *Corneal Contribution to the Wavefront Aberration of the Eye*. *School of Optometey*. Indiana University.

Statistics and data collections. *NHS The Information Centre*. Retrieved from www.ic.nhs.uk/statistics-and-data-collections/social-care/

Thibos, Larry N; Xiaofeng, Qi; Donald, M. T. Vision through a liquid-crystal spatical light modulator. *Vision Science Group*.

Visual Impairment and blindness. (n.d.).*World Health Organization*. Retrieved from http://www.who.int/mediacentre/factsheets/fs282/en/

Williams, Charles S; Becklund, O. A. (2002). *Introduction to the Optical Transfer Function* (First edit.). New York: SPIE- the international society for Optical Engineering.

Wilson, A. (1989). A review of the prevalence and causes of Myopia.

Wilson, R. . (2001). *Fourier Series and Optical Transform Techniques in Contemporary Optics: An Introduction*. (I. John Wiley and Sons, Ed.). New York.

Wyant, J. C. (1992). Basic Wavefront Aberration Theory for Optical Metrology. *APPLIED OPTICS AND OPTICAL ENGINEERING*, *11*(1), 1–53.

Zhao, S. E. (2007). Wavelength of Maximum Human Visual Sensitivity. *The Physics Factbook*. Retrieved from http://hypertextbook.com/facts/2007/SusanZhao.shtml

visual pathway. (2011).*eDoctoronline.com*. Retrieved from http://www.edoctoronline.com/medical-atlas.asp?c=4&id=21964

BIBLIOGRAPHY

Maheshwari, A., & Williams, D. (2001). Learning Optics using Vision. *Biomedical Engineering & Center for Visual Science at University of Rochester*. Retrieved from http://www.cfao.ucolick.org/EO/Resources/Learn_optics_AO.pdf

Dua, Sumeet; Archarya, Rajendra; Ng, E. Y. K. (2011). *Computational Analysis of The Human Eye with Applications* (First Edit., p. 468). Singapore: World Scientific Publishing Co. Pte. Ltd

Jr, M. A. (2006). A method for enhancing digital information displayed to computer users with visual refractive errors via spatial and spectral based processing. *ACM SIGACCESS Accessibility and Computing*, 22–25. Retrieved from http://dl.acm.org/citation.cfm?id=1127568

Jr, M. A., & Barreto, A. (2003). An Image Processing Approach to Pre-compensation for Higher-Order Aberrations in the Eye F. *SYSTEMICS, CYBERNETICS AND INFORMATICS*, *2*(3), 1–4.

Liang, J., Grimm, B., Goelz, S., & Bille, J. F. (1994). Objective measurement of wave aberration of the human eye with the use of Hartmann-Shack wave-front sensor, *11*(7).

Liang, J., Williams, D. R., & Miller, D. T. (1997). Supernormal vision and high-resolution retinal imaging through adaptive optics. *Journal of the Optical Society of America. A, Optics, image science, and vision*, *14*(11), 2884–92. Retrieved from http://www.ncbi.nlm.nih.gov/pubmed/9379246

M.A., Hogervorst; W.J.M., van D. (2006). Visualizing visual impairments. *Gerontechnology*, *5*(4), 208–221.

Ng, E. Y. K; Tan. Jen. Hong; Acharya. Rajendra; Suri. Jasjit (2012). *Human Eye Imaging and Modeling* (First edit., p. 430). Singapore: CRC Press.

Thibos, L. (2000). Formation and sampling of the retinal image. *Handbook of perception and cognition*, 1–87.

Wilson, A. (2012). Simulator aids design for the visually impaired. *PennWell Corporation*. Retrieved from http://www.vision-systems.com/blogs/vision-insider/2012/01/simulator-aids-design-for-the-visually-impaired.html

APPENDIX A

WAVE ABERRATION

When plane waves are incident on a curved optical system, the optical system will bend all the plane waves so they all focus at a point. If the surface of an optical system is not smooth, then they cause aberrations, thus plane waves are no longer focused and are vaguely bent; described by the function $W(x, y)$ - defined as the product of the refractive index and the optical path length of the plane wave (Wyant, 1992). It is measured with reference to spherical wavefront along the exit pupil with the transverse coordinates (x, y), shown in figure A-1.

Wave aberration can be expressed using Taylor expansion of polynomial with the pupil coordinates is shown in eq. (A.1),

$$\begin{aligned} W(r,\theta) = {} & W_{020}r^2 + W_{040}r^4 + W_{131}hr^3\cos\theta + W_{222}h^2r^2\cos^2(\theta) \\ & + W_{220}h^2r^2 + W_{311}h^3r\cos\theta \\ & + \cdots(higher\ order\ terms) \end{aligned} \tag{A.1}$$

where,
W_{klm} are the wave aberration coefficients for different modes
h is the height of the object
(r, θ) are the polar coordinates in the pupil plane

r^2	= Defocus
r^4	= Spherical Aberration
$hr^3\cos(\theta)$	= Coma
$h^2\ r2\ \cos2(\theta)$	= Astigmatism
$h^2\ r^2$	= Field Curvature
$h^3 r\cos(\theta)$	= Distortion
higher order terms	= Secondary, Tertiary, etc

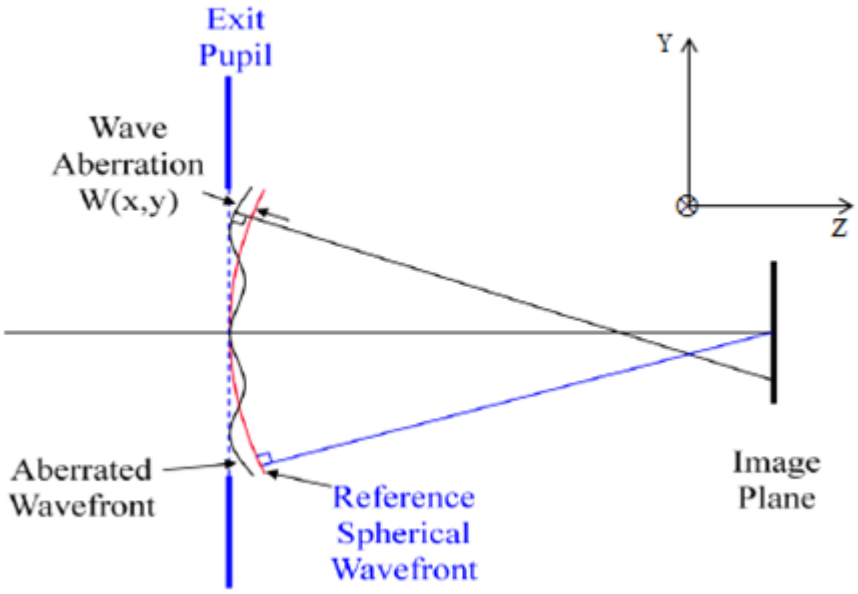

Figure A-1 Wavefront aberration from a distant object (Love, 2000).

Aberration has a negative effect on the quality of the image, they change the size, shape and the impulse response or point spread function of the image, which eventually blurs the image. Therefore, aberration can be characterised by calculating the PSF of the optical system, from eq. (5.22) the Point Spread Function of the eye can be evaluated.

ZERNIKE POLYNOMIALS

Waveform aberrations are written using Zernike polynomials; they form a set of functions that are orthogonal over a unit circle, therefore they are best suited for describing wavefront aberration. These polynomials are expressed in polar coordinates (ρ, θ) where $0 \leq \rho \leq 1$ and $0 \leq \theta \leq 2\pi$. Figure A-2, shows the coordinate system of Zernike polynomials on a unit circle, this can be converted into Cartesian coordinates. Since the polynomials are orthogonal, they are mathematically independent and are scaled such that they have unit variance and zero mean. The polynomials are normalised to have unit magnitude at the edge of the eye and the terms are normalised so that the coefficient of a particular term or mode is the RMS contribution of that term. The weighted sum of Zernike polynomials describes the wave aberration of the eye; eq. (A.2) gives the definition of Zernike polynomials.

$$Z_n^m(\rho,\theta) = \begin{cases} N_n^m R_n^{|m|}(\rho)\cos(m\theta) \text{ for } m \geq 0, 0 \leq \rho \leq 1, 0 \leq \theta \leq 2\pi \\ -N_n^m R_n^{|m|}(\rho)\sin(m\theta) \text{ for } m < 0, 0 \leq \rho \leq 1, 0 \leq \theta \leq 2\pi \end{cases} \quad \text{(A.2)}$$

Where, n, m can only take values from: $-n$, $-n+2$,$-n+4$,…,n

$$N_n^m = \sqrt{\frac{2(n+1)}{1+\delta_{m0}}} \qquad \delta_{m0} = 1 \text{ for } m = 0,\ \delta_{m0} = 0 \text{ for } m \neq 0 \quad \text{(A.3)}$$

Eq. (A.3) called the normalisation factor of Zernike polynomials.

$$R_n^{|m|}(\rho) = \sum_{s=0}^{\frac{(n-|m|)}{2}} \frac{(-1)^s (n-s)!}{s!\,[0.5(n+|m|)-s\,]!\,[0.5(n-|m|)-s]!}\rho^{n-2s} \quad \text{(A.4)}$$

An expression for Radial polynomials is shown in eq. (A.4).

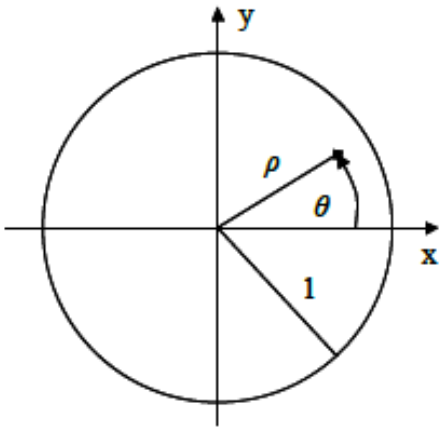

$$x = \rho \cos(\theta)$$
$$y = \rho \sin(\theta)$$
$$\theta = \tan^{-1}(x/y)$$
$$\rho = r/a = (x^2+y^2)^{1/2}$$

Figure A-2 Normalised Pupil Coordinate system using rectangular coordinates (Love, 2000).

The Shack-Hartmann wavefront are represented in Cartesian coordinates and the conversion from polar to Cartesian coordinates is given in eqs. (A.5), (A.6) and (A.7).

$$Z_n^m(\rho, \theta) \Rightarrow Z_n^m(x, y) \tag{A.5}$$

Using trigonometric identities and coordinate transformation of polar to rectangular coordinates:

$$x = \rho \cos\theta \ \& \ y = \rho \sin\theta \tag{A.6}$$

and

$$\rho = \sqrt{x^2 + y^2} \tag{A.7}$$

WAVE ABERRATION FUNCTION EXPRESSED USING ZERNIKE POLYNOMIALS

The weighted sum of Zernike polynomials are used to denote a wave aberration of the eye, represented in eq. (A.8),

$$W(\rho,\theta) = \sum_{n}^{k} \sum_{m=-n}^{n} W_n^m \, Z_n^m(\rho,\theta) \tag{A.8}$$

the above mathematical relation between wave aberration and Zernike coefficients can be expanded into its odd and even components, shown in eq. (A.9).

$$W(\rho,\theta) = \sum_{n}^{k} \left\{ \sum_{m=-n}^{-1} W_n^m \left(-N_n^m R_n^{|m|}(\rho)\sin(m\theta)\right) + \sum_{m=0}^{n} W_n^m (N_n^m R_n^{|m|}(\rho)\cos(m\theta)) \right\} \tag{A.9}$$

where, *k* gives the order of the polynomial expression

W_n^m gives the coefficients of Z_n^m in the expression

W_n^mgives the RMS wavefront error of that mode

For simplicity and computational purposes, eq. (A.9) can be re-written in rectangular coordinates and using only single index,

$$W\ (x,y) = \sum_{j=0}^{j\ max} W_j Z_j(x,y) \tag{A.10}$$

Where, $W_j = W_n^m$ and $Z_j = Z_n^m(x,y)$.

and;

$$j = \frac{n(n+2)+m}{2} \tag{A.11}$$

In this equation A.11, j max refers to the highest mode number included in the expression.